Published in final edited form as:
Expert Opin Drug Deliv. 2009 November ; 6(11): 1175–1194. doi:10.1517/17425240903229031.

Nanoparticles for biomedical imaging

Satish K Nune[1,†], **Padmaja Gunda**[2], **Praveen K Thallapally**[1], **Ying-Ying Lin**[3], **M Laird Forrest**[2], and **Cory J Berkland**[2,3]

[1]Energy and Environment Directorate, Pacific Northwest National Laboratory, 902 Battelle Boulevard, PO Box 999, MSIN K6-81, Richland, WA 99352, USA

[2]University of Kansas, Department of Pharmaceutical Chemistry, Lawrence, KS 66047, USA

[3]University of Kansas, Department of Chemical and Petroleum Engineering, Lawrence, KS 66045, USA

Abstract

Background—Synthetic nanoparticles are emerging as versatile tools in biomedical applications, particularly in the area of biomedical imaging. Nanoparticles 1 – 100 nm in diameter have dimensions comparable to biological functional units. Diverse surface chemistries, unique magnetic properties, tunable absorption and emission properties, and recent advances in the synthesis and engineering of various nanoparticles suggest their potential as probes for early detection of diseases such as cancer. Surface functionalization has expanded further the potential of nanoparticles as probes for molecular imaging.

Objective—To summarize emerging research of nanoparticles for biomedical imaging with increased selectivity and reduced nonspecific uptake with increased spatial resolution containing stabilizers conjugated with targeting ligands.

Methods—This review summarizes recent technological advances in the synthesis of various nanoparticle probes, and surveys methods to improve the targeting of nanoparticles for their application in biomedical imaging.

Conclusion—Structural design of nanomaterials for biomedical imaging continues to expand and diversify. Synthetic methods have aimed to control the size and surface characteristics of nanoparticles to control distribution, half-life and elimination. Although molecular imaging applications using nanoparticles are advancing into clinical applications, challenges such as storage stability and long-term toxicology should continue to be addressed.

Keywords

biomedical imaging; molecular imaging; nanoparticle synthesis; surface modification; targeting

1. Introduction

Nanotechnology has emerged as a multidisciplinary research effort aimed at understanding and manipulating materials by converging concepts from engineering, chemistry, biology, medicine and others [1]. Recent technological advances in the generation of diverse types of nanoparticle clearly exemplify the importance of nanoparticles in biological imaging applications [2,3]. According to the National Nanotechnology Initiative (NNI), nanoparticles have a diameter ranging from 1 to 100 nm. Within the biomedical community, slightly

[†]Author for correspondence: Tel: +1 509 371 6632; Fax: +1 509 371 7249; satish.nune@pnl.gov.

larger particles are often defined as nanoparticles as well, owing to a similarity in size to important naturally occurring nanoparticles such as viruses. At these dimensions, nanoparticles show unique properties that may be distinct from both molecules and bulk solids. Without the aid of exogenous targeting ligands, nanoparticles have been observed to target tumors passively through the enhanced permeability and retention effect (EPR) [4], or specific tissues such as the lymphatic system through molecular sieving [5]. On conjugation with tumor targeting ligands (e.g., peptides, small organic molecules, antibodies, etc.), nanoparticles can be successfully used as tumor-specific probes with high specificity [6]. Emerging nanoparticle technologies are joined by intense development of imaging modalities to assist with disease detection. Molecular imaging refers to the development of molecular probes for the visualization of the cellular function, characterization and the measurement of molecular processes in living organisms at the cellular and molecular level without perturbing them [7]. This review focuses on recent synthetic approaches in the development of probes for molecular imaging and highlights several *in vivo* studies that exemplify the efficacy of selected probes.

The use of engineered nanoparticles in biological investigations has increased exponentially in the last 5 years for a variety of reasons. At the nanometer scale, unique physical, chemical and optical properties have been discovered. As a result, new synthetic methods have been developed to control precisely the size and shape of nanoparticles as a means to tune absorption and emission properties. Concurrently, surface modification or 'biofunctionalization' of nanoparticles has leveraged the high surface-to-volume ratio to enable multivalent ligand binding to target biomolecules [8]. Many scientific applications are now being enabled through molecular targeting of nanoparticle beacons.

1.1 Nanoparticles in molecular imaging

At present, a variety of nanoparticle systems are being investigated to explore their potential in molecular imaging, with many applications aimed at diagnosis or treatment of cancer [9]. Particle charge, size, shape and hydrophilicity remain among the most important properties of nanoparticles for effective delivery to the desired target. Polyethylene glycol (PEG) molecules have been investigated extensively as an effective means to provide hydrophilic 'stealth' properties, commonly yielding reduced nonspecific adsorption of serum proteins *in vivo*, thus producing longer circulation times [10]. Conversely, positively charged nanoparticles are being designed for enhancing endocytosis or phagocytosis for cell labeling [11]. Various types of nanoparticle are now under investigation, including solid lipid nanoparticles, liposomes, micelles, nanotubes, metallic nanoparticles, quantum dots, dendrimers, polymeric nanoparticles and iodinated nanoparticles. This review mainly emphasizes four representative nanomaterials (gold nanoparticles, quantum dots, iron oxide nanoparticles and dendrimers) in biomedical imaging applications. There is also a brief discussion on other sundry nanoparticles.

Metallic nanoparticles possess immense potential as X-ray contrast imaging agents owing to their potent X-ray absorption and low toxicity profiles observed over short durations in animals [12,13]. Gold nanoparticles have gained significant attention owing to the potential biocompatibility, relatively low short-term toxicity, and high absorption coefficient and physical density compared with iodine (gold 79(Z), 5.16 cm^2/g, 19.32 g/cm^3; iodine 53(Z), 1.94 cm^2/g, 4.9 g/cm^3). Therefore, there is a significant demand for the synthesis of these types of nanoparticle under benign conditions that reduce concerns regarding the toxicity potentially induced by the reducing agents and reaction conditions.

Although there are many types of nanoparticle-based cancer therapeutics and molecular imaging agents available, many of them would benefit from improvements in specificity (e.g., for tumor cells), in *in vitro* and *in vivo* stability, and in prolonging the circulation half-

life [14,15]. The ability to target nanoparticles could present a significant improvement over current contrast media. The addition of targeting ligands provides a means to obtain high specificity and increased nanoparticle–tumor interactions for diseased tissues [16,17]. It is well documented that nanoparticles can be functionalized with various targeting ligands, including small molecules, peptides, proteins and antibodies [18,19], offering the potential for improved drug delivery and diagnosis of disease.

Many functionalized nanoparticles have been designed to have high affinity towards diverse cancerous cell surface receptor proteins that are overexpressed on a variety of cancer cells (Figure 1A) [16,17]. Although antibody-modified nanoparticles have found success in the labeling of cells and tissues, translating this technological development to clinical application may be very challenging because of their limited shelf-life and the high costs associated with synthetic functionalization of targeting peptides and antibodies. An alternative solution is to use small organic molecules that impart precise biological targeting. The multivalent presentation of small molecules may indeed be as a result of mediating relatively strong interactions between functionalized nanoparticles and the intended cells and biomolecules [18]. The use of small molecules as an alternative to antibodies allows further optimization of the binding affinity and specificity by adjusting the density of targeting molecules [18].

2. Synthesis and applications of nanoparticles for molecular imaging

2.1 Gold nanoparticles

Inorganic nanoparticles are emerging as versatile tools in imaging as a result of their unique chemical, physical and optical properties [20]. Gold nanoparticles were discovered > 100 years ago and, owing to their surface chemistry, projected biocompatibility, relatively low short-term toxicity, high atomic number and high X-ray absorption coefficient, gold nanoparticles have received significant interest recently for use in multiple imaging technologies. There are robust and facile synthetic methods for producing gold nanoparticles with precise control over the particle size and shape [21,22]. Gold nanoparticles can be synthesized under relatively benign conditions, which is important considering the emerging concerns about nanomaterial safety and toxicity for biomedical applications [21,23].

2.1.1 Synthesis—Spherical gold nanoparticles with sizes ranging from a few to several hundred nanometers can be synthesized conveniently in aqueous or organic solvents with a high degree of precision and accuracy [24]. In general, reduction of gold salts (e.g., $AuCl_4$-) leads to the nucleation of gold ions [25,26]. As gold nanoparticles are not stable, a stabilizing agent is required that is physically adsorbed or chemically bound to the gold surface. The generation of gold nanoparticles in aqueous medium typically uses either trisodium citrate or sodium borohydride as reducing agents [27,28]. Precisely controlling citrate concentration results in the formation of small and uniform gold nanoparticles.

2.1.2 Surface modification and bioconjugation—There are two approaches to functionalizing gold nanoparticles: ligand exchange of stabilizers and direct incorporation of a functional stabilizer. In the ligand exchange method, biomolecules containing functional groups such as thiols replace the stabilizer used during synthesis [24]. In the second method, biomolecules can be conjugated to the stabilizer molecules, which are already present on gold nanoparticles. Often the amino acid end groups of the stabilizer are modified by covalent conjugation of ligands, for example, by using EDC (1-ethyl-3-(3-dimethylaminoproply carbodiimide-HCl) chemistry [29,30]. Gold nanoparticles may also be generated in the presence of tumor-specific biomolecules, thus physically or chemically incorporating the biomolecule as part of the gold nanoparticle. The properties of the targeting ligand or stabilizer on the nanoparticle greatly influence the particle size, size

distribution and the polydispersity of metal nanoparticles [16,31]. Biocompatibility is an important constraint in utilizing gold nanoparticles for *in vivo* imaging applications. Therefore, the development of stable functionalized nanoparticles that specifically target cancer sites has received considerable attention.

2.1.3 Gold nanoparticles in biomedical imaging (computer tomography)—X-ray computer tomography (CT), is a commonly used diagnostic imaging tool offering broad availability and relatively modest cost. X-ray CT is used to visualize tissue density differences that provide image contrast by X-ray attenuation between soft tissues and electron-dense bone. It is desirable to enhance the contrast of diseased tissue with the use of X-ray contrast agents to increase the contrast between normal and cancerous tissue [12]. At present, highly water-soluble small organic iodinated molecules are typically used as CT contrast enhancers. These tend to suffer from very short imaging times owing to rapid renal clearance and nonspecific vascular permeation [12,32,33].

Hainfeld *et al.* demonstrated the use of gold nanoparticles (1.9 nm) as an X-ray CT contrast agent to detect tumors in mice [13]. The injected gold nanoparticles were not detected in the blood after 24 h, but showed significant accumulation in the kidney (10.62% injected dose/g [ID/g]), the tumor (4.2% ID/g), liver (3.6% ID/g) and muscle (1.2% ID/g) after just 15 min. The gold nanoparticles were cleared through the kidneys by means of renal excretion and did not concentrate in the liver or spleen, presumably because of the small size of the nanoparticles. Recently, Kattumuri *et al.* successfully demonstrated the use of gum Arabic stabilized gold nanoparticles as a potential biocompatible X-ray CT contrast agent [34]. Limited binding of the nanoparticles with blood plasma suggested *in vivo* stability of the nanoparticles. Kim *et al.* recently developed PEG-coated gold nanoparticles to impart anti-biofouling properties to extend the systemic circulation half-life. PEG-coated nanoparticles injected intravenously into rats showed much longer blood circulation time (> 4 h) than the commonly used iodine contrast agent iopromide (< 10 min) [35]. Using X-ray CT, the authors also showed that intravenous injection of PEG nanoparticles into hepatoma-bearing rats produced enhanced contrast (approximately twofold) between hepatoma and normal liver tissue. These PEG-coated nanoparticles were synthesized using the ligand exchange method. Gold nanoparticles were produced by the reaction of $HAuCl_4$ with sodium citrate. The ligand exchange reaction was performed by mixing the citrate-gold nanoparticles with PEG-SH and stirring for 1 h to modify covalently the gold nanoparticles with PEG.

Until recently, CT generally was not considered to be a molecular imaging modality like magnetic resonance imaging (MRI) and various other nuclear medicine imaging modalities (single-photon-emission computed tomography [SPECT], positron-emission tomography [PET], etc.). Popovtzer *et al.*, however, demonstrated the use of gold nanoparticles as target-specific agents to detect head and neck cancer *in vitro* with a standard clinical CT [16]. The authors used gold nanorods instead of spherical gold nanoparticles. It is important to note that in CT imaging, the amount of the gold content per unit volume is important irrespective of particle shape and size. Squamous cell carcinoma (SCC) was selectively targeted with gold nanorods with conjugated UM-A9 antibodies. Gold nanorods were synthesized by the method of Nikoobakht and El-Sayed [36]. UM-A9 antibody was conjugated to polyacrylic acid (PAA) adsorbed to the gold nanorods using EDC/NHS chemistry. Antibody-coated gold rods were then mixed with the cancer cell suspension for 1.5 h, washed and redispersed and CT scans were obtained using a clinical CT operating at 80 kVp. The authors successfully demonstrated that the A9-antibody-coated gold nanorods targeted the SCC cells and showed an increased attenuation coefficient (ΔHU; 168 – 170) compared with non-targeted nanorods, non-cancerous cells (normal fibroblast cells) and other cancerous cells (melanoma) (ΔHU; 28 – 32). The increased X-ray attenuation in targeted SCC cells

compared with normal cells substantiates the basic premise for the development of molecular X-ray CT imaging agents (Figure 1B) [16].

2.1.4 Gold nanoparticle-based colorimetric biosensing—Gold nanoparticles have also emerged in diagnostics as colorimetric biosensors [37]. The assay is based on a change in color resulting from a change in the plasmon resonance frequency. The plasmon resonance frequency depends on the average distance between gold particles. For example, during the formation of gold agglomerates, the color may change from red to purple or blue. During redispersion of gold agglomerates, the reverse color change from purple to red color was often observed. Mirkin and co-workers pioneered the use of this phenomenon with the development of DNA-gold sensors [38,39]. Also, the plasmon resonance frequency depends on the aspect ratio of the nanoparticles, for example nanorods with high aspect ratios have resonances at lower frequencies. At present, this methodology is used for the detection of various biomolecules, including peptides, metals (e.g., mercury or lead), small molecules and nucleic acids [40-43]. Typically, gold nanoparticle biosensing is based on the interaction of a crosslinker with a receptor molecule on nanoparticles or on the interaction between nanoparticles containing receptors when an anti-receptor is added [38].

2.2 Quantum dots

Quantum dots (QDs) are fluorescent semiconductor nanocrystals (~ 1 – 100 nm) with unique optical and electrical properties [8,14,44]. Compared with organic dyes and fluorescent proteins, QDs possess near-unity quantum yields and much greater brightness than most dyes (10 – 100 times). Quantum dots also show broad absorption characteristics, a narrow linewidth in emission spectra, continuous and tunable emission maxima due to quantum size effects, a relatively long fluorescence lifetime (5 to > 100 ns compared with 1 – 5 ns in organic dyes) and negligible photobleaching (100 – 1000 times less than fluorescent dyes) over minutes to hours [45]. These properties make QDs advantageous for medical imaging applications when paired with the potential for *in vivo* targeting of specific cells (e.g., labeling neoplastic cells, DNA, and cell membrane receptors) after conjugation with specific bioactive moieties. One drawback is the blinking phenomenon observed in these semiconductors. Synthetic techniques exist for the precise control of QD size and composition, which in large part control the absorption and emission characteristics. This can allow researchers to exploit QDs' unique properties for applications such as cell labeling, biosensing and nucleic acid detection. Applications of QDs are predicted to grow because of advantages over other biological labeling methods (e.g., fluorescent dyes and radioisotopes) [14,44,46,47].

2.2.1 Synthesis—Quantum dots have a synthetic history of ~ 17 years, with synthesis described by Ekimov and Onuschenko and Efros and Efros in 1982 [48,49]. Extensive effort has been invested ever since to enlarge the spectrum, functionality and biocompatibility of QDs. Quantum dots, like any other nanoparticles, have a large number of atoms on the surface containing vacant atomic or molecular orbitals. Bawendi and co-workers developed a synthetic method for the synthesis of QDs containing cadmium sulfide (CdS), cadmium selenide (CdSe), or cadmium telluride (CdTe) [50]. Quantum dots have been developed with a metalloid crystalline core (e.g., CdSe) and a shell (e.g., ZnS) that shields the core. It was assumed that the capping of QDs with wider band gap semiconducting materials such as zinc sulfide (ZnS) would improve the photoluminescence efficiency [51-53]. Use of ZnS capping also decreases the oxidative photobleaching of QDs [53,54] and greatly enhances the surface binding properties of CdS, CdSe and CdTe-core QDs to ligands such as phosphines and amines, thereby improving colloidal stability [51,55].

Although methods for the synthesis of QDs in aqueous medium have been developed, these methods have rarely yielded colloidal stability with high monodispersity compared with QDs generated in the presence of coordinating hydrophobic ligands. In a typical shell growth method for the synthesis of QDs, a selenium precursor (e.g., trioctylphosphine (TOP)-selenide) is added rapidly to a hot solution of a cadmium precursor (e.g., cadmium oleate) and a coordinating ligand (e.g., hexadecylamine) under inert atmospheric conditions followed by the addition of a solution of diethyl zinc. Hexamethyldisilathiane in TOP is then added slowly to improve the photoluminescence efficiency. Purification using liquid–liquid extraction or precipitation leads to the recovery of pure (CdSe)ZnS nanocrystals [8]. The selection of QD core composition is dictated by the desired wavelength of emission.

2.2.2 Surface modification and bioconjugation—The necessity of hydrophobic conditions for synthesis of high-quality QDs impedes direct transfer to biological applications, as many biomolecules have limited solubility and stability in organic solvents [52,56,57]. Similar to gold nanoparticles, ligand exchange or conjugation to surface stabilizers can be used for surface modification of QDs to improve stability in aqueous conditions and biocompatibility [8,24]. In the ligand exchange process, heterobifunctional ligands such as mercaptoacetic acid or 3-mercaptopropyl trimethoxy silane containing thiol functionalities are used, which can covalently bind to QDs. The acid functionalities improve QD hydrophilicity [58]. However, the ligand exchange method may induce agglomeration and decrease fluorescence efficiency. Another approach to improve the stability and solubility in aqueous conditions is surface stabilization using amphiphilic polymers [59,60]. Modified QDs with increased water stability may then be conjugated with specific ligands such as peptides, antibodies or small molecules to impart target specificity [61-64]. Similar to gold nanoparticles, PEG can be conjugated to QDs potentially to extend the blood circulation time and reduce nonspecific binding to serum proteins in blood [65].

2.2.3 Quantum dots in biomedical imaging—Quantum dots are increasingly used as fluorophores for *in vivo* fluorescence imaging. Fluorescence imaging has several advantages compared with other imaging modalities because this method has good sensitivity and is non-invasive in nature, using readily available and relatively inexpensive instruments. Being an optical technique, it is limited in terms of tissue penetration depth. A wide variety of *in vivo* studies have validated the potency of QDs. Akerman *et al.* have demonstrated significant accumulation of CdSe/Zns QDs coated with PEG and a lung-targeting peptide in the lungs of mice [66]. Gao *et al.* recently described the development of multifunctional nanoparticle probes based on QDs for *in vivo* imaging of human prostate cancer in mice. This new class of coated QDs is based on the encapsulation of PEGylated QDs using an ABC triblock copolymer as a secondary coating layer, further functionalized with a tumor-targeting antibody to prostate-specific membrane antigen [44]. Cai *et al* used peptide-conjugated QDs for non-invasive, targeted *in vivo* imaging of tumors (Figure 2A). They showed that QDs labeled with arginine-glycine-aspartic acid (RGD) peptide selectively target the $\alpha_v\beta_3$-positive tumor vasculature in a murine xenograft model, as observed from near infrared (NIR) fluorescence images [67]. Although there was significant accumulation in the liver, bone marrow and lymph nodes, 6 h after the injection of QDs, high tumor contrast was also observed (Figure 2B) [67]. Ballou *et al.* studied the localization of four QDs with different surface coatings and demonstrated that the QDs remained fluorescent for at least 4 months *in vivo* and that the localization of QDs was dictated by the surface coating [68]. Kim *et al.* developed near infrared fluorescent type II QDs for sentinel lymph node mapping [69,70]. In normal QDs (type I), the shell material is made of high band gap material where the conduction band is of higher energy than the core and the valence band of the shell is lower than that of the core. By contrast, type II QDs are composed of core–shell materials with offset band gaps. Recently, Tada *et al.* has tracked single QDs coated

with monoclonal anti-HER2 antibody in tumors of living mice in the dorsal skinfold chamber using a high-speed confocal microscope [71]. Gao *et al.* recently developed a QD-based contrast agent for brain imaging. The agent was based on surface modification of QDs using poly(ethylene glycol)-poly(lactic acid), which was then functionalized with wheat germ agglutinin. The QD-based imaging agent was delivered to the brain by means of intranasal administration [72]. The QDs accumulated in the brain for > 4 h and were cleared 8 h after administration.

Careful incorporation of multiple components such as gadolinium and manganese in QDs allows creation of multimodal imaging agents [73]. Working in this direction, Jin *et al.* developed hybrid QDs with the careful integration of Gd^{3+} in QDs to achieve dual mode (fluorescence/magnetic resonance) imaging. The hydrophobic NIR-QDs (CdSeTe/CdS) were functionalized with glutathione to improve biocompatibility and then functionalized further with Gd^{3+}-DOTA (DOTA: 1,4,7,10-tetraazacyclododecane-1,4,7,10-tetraacetic acid) [74]. Similarly, Yong developed a new approach to produce manganese-doped QDs as multimodal targeted probes for pancreatic cancer imaging. Confocal spectroscopy was used to determine the localization of anti-claudin, anti-mesothelin, or anti-PSCA-coated QDs to pancreatic cancer cells [73].

2.3 Iron oxide nanoparticles

Magnetic nanoparticles have received considerable attention because of their potential use in optical, magnetic and electronic devices [1,13,75,76]. Similar to gold nanoparticles and QDs, metal nanoparticles of iron oxide are expected to show acceptable biocompatibility at low concentration, high magnetic saturation and functional surfaces. Magnetic iron oxide nanoparticles have been functionalized with antibodies, nucleosides, proteins and enzymes for directing them to diseased tissues such as tumors [77,78]. Iron oxide nanoparticles show superparamagnetism and high field irreversibility, which arise in part from the size and surface properties of individual nanoparticles [75,79]. For more than two decades, magnetic nanoparticles have been used successfully clinically [80-82]. The chemical and structural design of magnetic nanoparticles is similar to gold nanoparticles and QDs. Highly superparamagnetic iron oxide is commonly used as the core material, and biocompatible polymers such as dextran may be used as a coating material [83]. Superparamagnetic iron oxide nanoparticles (SPION) have large magnetic moments and are well suited as T2 contrast agents in MRI. *In vivo*, SPIONs may be directed to the reticuloendothelial system (RES) [84,85] as determined by the particle size and surface chemistry. SPIONs are further classified into crosslinked iron oxide nanoparticles (CLIO) [86], large SPIO (iron oxide nanoparticles with polymer coating materials) and ultra-small SPIO [87,88].

2.3.1 Synthesis—There has been substantial interest in obtaining iron oxide nanoparticles with controlled shapes and sizes for reasons mentioned previously. To meet this challenge, several synthetic approaches have been developed, including microemulsion [89], sol-gel [90], sonochemical synthesis [91] and co-precipitation techniques [92,93]. Aqueous co-precipitation of nanoparticles in the presence of a coating material appears to be the most common method. Methods that use hydrophobic ligands and organic solvents report precise control over the particle size and shape. To improve biocompatibility, water-insoluble nanoparticles may be fabricated with a multifunctional ligand system (e.g., 2,3-dimercapitosuccinic acid [DMSA]) that enables the transfer of nanocrystals to an aqueous phase [94]. Recent improvements in the synthetic methods for magnetic nanoparticles include improved control over the particle size in aqueous environments, dramatic increases in magnetic resonance contrast, and inclusion of functional groups that facilitate the attachment of biomolecules [82]. Mohammadi *et al.* recently reported a new co-precipitation method to synthesize iron oxide within a suspension of polyvinylamine nanoparticles, which

yielded a stable colloid with reactive primary amines [95]. The most studied parameter of magnetic nanoparticles is particle size, owing to its critical role in contrast enhancement [82]. Recently, Jun *et al.* demonstrated the effect of size on the magnetism and magnetic resonance enhancement properties of Herceptin-conjugated magnetic nanoparticles [96]. They showed that the mass-magnetization of nanoparticles at 1.5 T was 25, 43, 80 and 101 e.m.u./(g Fe) for particles of 4, 6, 9 and 12 nm, respectively (Figure 3A) [96]. By discretely increasing particle size, T2-weighted contrast was enhanced dramatically.

The magnetic properties of iron oxide nanoparticles may be improved further by doping with other metals. Typically, nanoparticles are doped to produce MFe_2O_4 (M = Mn, Fe, Co or Ni), where the Fe^{2+} in Fe_3O_4 is replaced with metal 'M' [97]. Recently, Lee *et al.* synthesized various metal-doped ferrite nanoparticles (MFe_2O_4) and demonstrated that $MnFe_2O_4$ nanoparticles have higher magnetic susceptibility compared with other divalent metal dopants [98]. Also, it is very important to note that these nanoparticles and their conjugates are non-toxic at examined concentrations, ~ 200 μg/ml. These metaldoped ferrite nanoparticles with increased magnetic resonance contrast may be useful as ultrasensitive MRI probes [98].

2.3.2 Surface modification and bioconjugation—As with other nanoparticles, surface coatings of iron oxide nanoparticles affect the performance of the nanoparticles *in vivo*. Coatings may reduce uptake by the RES, increase circulation half-life and improve accumulation in target tissues. Polymers (e.g., dextran) are commonly used as coating materials to improve biocompatibility and stability [80,83]. Also, coating of monomeric molecules such as DMSA, bisphosphonates and alkoxysilanes has been described [80,94]. Similar to other nanoparticles, coating iron oxide nanoparticles with PEG increases the colloidal stability and circulation half-life *in vivo* [99,100]. Polymers containing terminal bifunctional ligands have been used to increase colloidal stability (Figure 4A) [101]. Multidentate polymeric ligands such as triethoxysilyl-terminated PEG ligands have been reported to increase the colloidal stability [102]. Sun *et al.* have developed conjugation strategies for the creation of magnetofluorescent nanoparticle libraries. Various small molecules such as diglycolic anhydride, glucosamine, digoxigenin, folic acid, cysteine-containing HA peptide and glycidoxypropyltrimethoxy silane with various reaction functionalities (anhydride, amino, hydroxyl, carboxyl, thiol and epoxy) have been covalently linked to amino-CLIO-FITC nanoparticles (Figure 4B; FITC: fluorescein isothiocyanate) [103].

2.3.3 Iron oxide nanoparticles in biomedical imaging (magnetic resonance imaging)—MRI is a non-invasive medical imaging technique that is commonly used in clinical medicine to visualize the structure and function of tissues [7,82,104], and generally provides increased contrast between soft tissues compared with computer tomography (X-ray CT). MRI is based on the behavior, alignment and interaction of protons in the presence of an applied magnetic field. Within a strong magnetic field, protons in the tissue are perturbed from B_0; contrast agents are used to alter longitudinal (T1) or transverse (T2) relaxation times, which can be monitored by MRI. Contrast agent efficiency is determined by its relaxivity over a range of concentrations. Unlike radionuclide-based imaging, MRI eliminates the radiation dose and can offer higher spatial resolution [7,82,105].

Several nanoparticles have been developed to improve contrast in MRI imaging. A significant benefit associated with iron oxide nanoparticles is their biocompatibility, and ready detection at moderate concentrations. SPIONs have a high saturation magnetization and loss of magnetization in the absence of magnetic field, and these nanoparticles are perceived to be relatively less toxic than optical imaging agents. Peptides, antibodies, proteins and small molecules have been conjugated to SPIONs and CLIOs for active

targeting [86]. Wunderbaldinger *et al.* used dextran-SPION to detect lymph node metastases in an experimental murine model using contrast-enhanced MRI [86,106]. Lewin *et al.* have described the synthesis of CLIO-TAT peptide conjugates (TAT, HIV transactivator of transcription), where the TAT peptide enhances the membrane translocating properties [107]. CLIO-TAT-labeled T cells have been used to visualize adoptive transfer of autoimmune diabetes in a mouse model [107]. Iron oxide-labeled cells have been observed to home selectively to specific antigens of B16 melanoma in a mouse model [108]. Kircher *et al.* used magnetofluorescent (CLIO-Cy5.5) nanoparticles delivered by means of tail vein injection as a preoperative MRI contrast agent and intraoperative optical probe for brain tumors using a xenograft model of gliosarcoma [109]. Recently, Montet *et al.* used magnetofluorescent nanoparticle conjugates targeting normal tissue in order to visualize tumors better. Bombesin (BN)-labeled magnetofluorescent nanoparticles targeting bombesin receptors present on normal acinar cells of the pancreas lead to a decrease in the T2 signal of normal pancreas tissue, thus enhancing the ability to visualize tumors by MRI [110]. Schellenberger *et al.* developed Annexin-V-labeled CLIO that recognized the phosphatidylserine of apoptotic cells at very low concentrations of nanoparticles [111]. Hu *et al.* developed magnetite nanocrystals (Fe_3O_4) labeled with surface-reactive αω-dicarboxyl-terminated PEG (HOOC-PEG-COOH) as the surface capping agent. Free terminal carboxyl groups were modified further with anti-carcinoembryonic antigen (CEA) monoclonal antibody rch 24 (rch 24 mAb), a cancer-targeting antibody. The biocompatible conjugates were used for MRI detection of human colon carcinoma in murine xenografts [112].

MRI has been used extensively to study the migration of cells (cellular trafficking) with magnetic nanoparticle probes [113,114]. Xie *et al.* synthesized c(RGDyK)-conjugated ultra-small iron oxide nanoparticles (USPION) for specific targeting to integrin $\alpha_v\beta_3$-rich tumor cells. USPIONs have been used to overcome nonspecific uptake, clearance, and to enhance extravasation in tumors [115]. Huh and co-workers developed well-defined iron oxide nanoparticles conjugated with Herceptin to image breast cancers by MRI. Herceptin binds specifically to the HER2/neu receptor, which is overexpressed in some breast cancer cells (Figure 3B) [98,116]. Recently, Lee *et al.* used Mn-doped iron oxide nanoparticles for ultrasensitive molecular imaging [98]. Engineered nanoparticles that possess high and tunable magnetism offer improved sensitivity and lower dosing compared with conventional iron oxide contrast agents. It is very important to note that Mn-doped nanoparticles are biologically non-toxic on two different cell lines (HeLa and HepG2).

2.4 Carbon nanotubes

The unique optical, electrical and mechanical properties of carbon nanotubes (CNTs) have attracted dramatic attention since their discovery by Iijima in 1991 in the soot of an arc discharge apparatus [117]. A variety of closed graphitic structures, including nanotubes and nanoparticles, were observed for the first time. CNTs are analogous to a monolayered graphite sheet rolled into tubes. Both single-walled and multi-walled structures can be produced. Extraordinary characteristics of CNTs, including high electrical and thermal conductivity and great tensile strength, indicate the potential for CNT use as field emission devices, tips for scanning microscopy, nanoscale transistors, or components for composite materials. The possibilities of using CNTs for biomedical applications are now under investigation. Current trends in biomedical imaging have focused on the NIR fluorescence properties of single-walled carbon nanotubes (SWNT) and on surface functionalization. NIR fluorescence lies in the biologically transparent region (700 – 1300 nm) where autofluorescence, absorption and scattering by blood and tissue are minimized. The unique NIR fluorescence properties of SWNTs [118] make SWNTs appealing as imaging contrast

agents [119,120] and biological sensors [121]. Surface functionalized multi-walled carbon nanotubes (MWNTs) have also been used successfully for bioimaging purposes [122].

2.4.1 Synthesis—Several methods, such as arc discharge and evaporation [117], laser ablation [123] and chemical vapor deposition (CVD) [124], have been developed for CNT production. Among these methods, the CVD method has been widely used for CNT production in recent years. Although the laser ablation technique is not amenable at present for scale-up, it is able to produce SWNTs with a purity as high as 90%. The arc discharge evaporation method is arguably the easiest and most common way to produce CNTs. In this method, CNTs are produced by means of arc evaporation of two carbon rods (10 or 20 mm in diameter) placed end to end with a 1 mm distance in an inert gas environment at 50 – 700 mbar. The two carbon rods are evaporated by direct current. The anode evaporates and rod-shaped tubes deposit on the cathode.

The reaction conditions and mechanisms of laser ablation are similar to the arc discharge method. A pulsed or continuous laser is used to vaporize a graphite target at 1200°C in an oven [123]. Inert gas (i.e., helium or argon) fills the oven, keeping the pressure at 500 torr. This method produces a high yield of SWNTs with narrow size distribution. In the CVD approach, a feedstock, for example hydrocarbon or CO, is heated to 800 – 1000°C with a transition metal catalyst to promote the growth of tubes. A two-step process occurs where catalyst is deposited on substrate and then the carbon source is placed in a gas phase reaction chamber.

2.4.2 Comparison between SWNT and MWNT—A SWNT is a rolled-up graphene sheet that is composed of benzene-type hexagonal rings of carbon atoms, whereas a MWNT contains a stack of graphene sheets rolled up into concentric cylinders. Both SWNT and MWNT have high mechanical strength [125] and high thermal and electrical conductivity. SWNTs show even more unique electronic properties in that they can be metallic or semiconducting depending on their chirality. Furthermore, SWNTs emit NIR fluorescence and the fluorescence is sensitive to the environment (i.e., pH, temperature and the existence of oxidant), which makes SWNTs good candidates for biomedical applications.

2.4.3 Carbon nanotubes for biomedical imaging—Applications of CNTs in biomedical imaging have recently emerged and are rapidly expanding. The major drawbacks of CNTs are their insolubility in many types of solvent and the concern that CNTs may exert harmful effects on organisms. However, it has been proved that surface functionalized CNTs (f-CNTs) can be highly soluble in water and can form supramolecular complexes with biological macromolecules and substrates based on electrostatic interactions [11]. No cytotoxicity was reported when SWNTs were used to shuttle various cargoes across cellular membrane [126].

A few bioimaging applications using CNTs have been developed for cancer cell destruction, detection and dynamic imaging. SWNTs covalently linked to visible-wavelength fluorophores have been imaged in cells using confocal microscopy [119,120]. Kam *et al.* [119] found the uptake of SWNTs and SWNT–streptavidin conjugates into human promyelocytic leukemia cells and human T cells by confocal microscopy. Pantarotto *et al.* [120] prepared FITC-labeled SWNTs by mixing amino-modified SWNTs with FITC in dimethylformamide. The capacity of the FITC-labeled SWNTs to penetrate into cells was studied using epifluorescence and confocal microscopy. Clear images from epifluorescence and confocal microscopy demonstrated that the f-CNTs were able to cross the cell membrane. Also, Sirdeshmukh and Panchapakesan used immunoglobulin G functionalized fluorescently tagged CNTs and confocal microscopy to prove the feasibility of developing a nanobioelectronic device that was specific to cell surface receptors in cancer cell [127].

Cherukuri *et al.* successfully used pristine SWNTs, spectrofluorometer and a fluorescence microscope modified for NIR imaging to study the cytotoxicity of SWNTs ingestion [128]. The fluorescence detection and imaging of SWNTs provide a powerful tool for tracing the interactions of SWNTs with tissues, cells and organisms.

Recently, the first report using MWNT for dynamic imaging was presented by Lacerda *et al.* [122]. In their study, MWNTs were functionalized with diethylentriaminepentaacetic dianhydride (DTPA-MWNT) and radiolabeled with indium-111 (^{111}In). The circulation of DTPA-MWNTs was dynamically tracked *in vivo* using a microSingle Photon Emission Tomography (microSPECT) scanner. Urinary excretion of DTPA-MWNT was confirmed at 24 h post-administration. The results of this study provide some support for using MWNT as components of therapeutic modalities and diagnostics in systemic indications.

2.5 Dendrimers

Dendrimers are well-defined, highly branched molecules that are synthesized with precise structural control and low polydispersity [129-132]. Tunable variation in size, the availability of a large number of reactive sites, and interior void space make dendrimers promising particulate systems for biomedical applications [129]. By taking advantage of the regular, structured nature of dendrimers, many of the obstacles associated with low-molecular-mass contrast agents and imprecise synthetic polymers can be overcome [129-133].

2.5.1 Synthesis—Dendrimers are synthesized in a stepwise manner either by the ‘divergent’ or the ‘convergent’ method. The divergent method, introduced by Tamalia, begins with a multifunctional core followed by repeated addition of monomers to increase molecular mass and exponentially increase surface termini [134]. As the generation of dendrimers increases, the chance of the incomplete derivatization also increases, resulting in imperfect dendrimers, which are very difficult to purify. Compared with any other method, divergent synthesis is easier, and in fact this approach is used to construct almost all of the commercially available dendrimers. By contrast, the convergent method pioneered by Hawker and Frechet begins from the surface and proceeds inward to a multivalent core where the dendrimer segments are joined together [135]. The main advantage of this method is that the growth of each dendrion can be carefully controlled; however, the final coupling step may be difficult to execute owing to steric hindrance. Dendrimer branching offers advantages such as precise nanometer-scale spherical structures (for high generations), low viscosity compared with an equivalent molecular mass of linear polymers, narrow polydispersity, and a high density of reactive sites. Over the past three decades, dendrimers such as polyamidoamine (PAMAM, i.e., Starburst™) and poly(propyleneimine) (PPI) with either a diaminobutane (DAB) or a diaminoethane (DAE) core have been explored as vehicles for drug or gene delivery and, more recently, as agents for biomedical imaging [129,136].

2.5.2 Dendrimers in biomedical imaging—Magnevist, a gadolinium(III)-diethylenetriaminepentaacetic acid (Gd-DTPA) complex, is a commonly used contrast agent for MRI, although rapid clearance and nonspecificity hinders its utility. Wiener *et al.* first reported gadolinium-PAMAM Starburst dendrimers as MRI contrast agents [137]. Initial studies of dendrimer-gadolinium polychelates probed the effect of physical parameters such as size and charge on circulation and disposition [129,130]. Dendrimer-based contrast agents demonstrated longer half-lifes than Gd-DTPA. For example, dendrimer contrast agents with molecular masses of 8508 and 139,000 Da had half-lifes of 40 ± 10 and 200 ± 100 min, compared with 24 ± 4 min measured for Gd-DTPA [137,138]. The overall performance of dendrimer-based contrast agents was dictated by the size, which influenced the

pharmacokinetics, permeability, clearance and RES uptake. Bryant *et al.* demonstrated a relationship between molecular relaxivity and molecular masses in Gd-DOTA-PAMAM dendrimers. Higher molecular mass dendrimers showed increased molecular relaxivity [138]; however, retention of ~ 40% of the contrast agent in the liver even after 7 days posed a significant challenge. Kobayashi *et al.* showed that different sizes yielded significant variations in blood retention, relaxivity and clearance rates [139]. Recently, Langereis *et al.* have evaluated various Gd-DTPA-terminated poly(propylene imine) dendrimers as contrast agents. Dynamic contrast-enhanced MRI revealed that G0 and G1 dendrimers showed rapid clearance and accumulated in the bladder. By contrast, G3 and G5 dendrimers were cleared at a much lower rate (Figure 5A) [133].

Targeted dendrimers for biomedical imaging have also been explored. Folic acid [140-142], antibodies [143] and proteins [144] have been incorporated onto the periphery of dendrimers to endow target specificity; however, only a few of them have been used in molecular MRI. Konda *et al.* developed and used folate-containing Gd-DTPA-PAMAM dendrimers (G4) as contrast agents. MRI studies in mice revealed a significant signal enhancement of ovarian tumors expressing folate receptor compared with mice with folate receptor-negative tumors [145]. Recently, Swanson *et al.* developed folic acid-containing Gd-DOTA-PAMAM (G5) (PAMAM-G5-FA) dendrimers for targeted, tumor-specific magnetic contrast enhancement [146]. MRI studies revealed that the PAMAM-G5-FA binds specifically to xenograft tumors established with human epithelial cancer cells that overexpressed folate receptor. Significant signal enhancement was observed in tumors when compared with non-targeted PAMAM-G5. Finally, Shi *et al.* recently developed a unique method for the development of folic acid-labeled dendrimers containing shell crosslinked iron oxide nanoparticles by combining layer-by-layer self-assembly and dendrimer chemistry [76].

3. Miscellaneous nanoparticles emerging in molecular imaging

3.1 Polyelectrolyte complex nanoparticles

Polyelectrolyte complex (PEC) nanoparticles are formed by electrostatically assembling two oppositely charged polymers [147-149]. The formation of the PEC nanoparticles is dictated by the strength of electrostatic interactions, size of the polyelectrolytes, pH and ionic strength of the reaction medium [150,151]. Polyelectrolyte capsules were produced by De Geest *et al.* [147] and Decher [152] using a layer-by-layer (LBL) technique by self-assembly of oppositely charged species on a colloidal substrate. Hartig *et al.* developed non-toxic PEC nanoparticles and evaluated toxicity, binding and internalization using endothelial cells [153]. The PEC nanoparticles are typically reported to be non-toxic compared with the precursor polyelectrolytes, but long-term toxicity is less well known, especially when non-degradable polyelectrolytes are used. PEC nanoparticles can be synthesized at room temperature using water as a solvent, thus circumventing the use of heat, organic solvents, initiators and surfactants, which are commonly used in polymer-based nanoparticle synthesis [147-149,152,154-156].

Polyelectrolyte complex nanoparticles have attractive properties for imaging and drug delivery. Careful selection of polyelectrolytes can produce PECs with water solubility, biodegradability and low toxicity [148]. PECs have been established as potential materials for gene delivery because of their relatively efficient transfection efficiency and simple formulation [147-149]. More recently, these nanocarriers have proved effective for entrapping and delivering small molecules, peptides, RNAs and even large proteins [149,157-159]. Although there is significant progress in the development of PECs as therapeutic agents, few reports are available on their use in biomedical imaging applications [156,160]. Fluorescent probes such as AlexaFluor 750 (AF 750) have been incorporated in low-molecular-mass poly(methylene-*co*-guanidine) hydrochloride (PMCG) PEC

nanoparticles for *in vivo* applications [148]. Huang *et al.* developed a PEC nanoparticle contrast agent for MRI. Gadolinium was incorporated in PEC nanoparticles by means of Gd-DTPA grafting to chitosan and ionic trapping of Gd ions. MRI studies revealed that contrast-enhanced PECs rapidly accumulated in the rat kidney with some accumulation in the liver [160].

3.2 Calcium phosphate nanoparticles

Calcium phosphate nanoparticles have received attention because of reports of low toxicity, biocompatibility and solubility in cells [161-165]. Calcium phosphate has been used as a delivery vehicle for DNA [166-168] and has been studied as a nanoparticle for gene delivery [161,162]. Also, these particles have been used for the encapsulation of organic molecules, fluorescent dyes and chemotherapeutic drugs, suggesting the potential for *in vivo* biomedical imaging and drug delivery applications [163-165]. Recently, Altinoglu *et al.* developed calcium phosphate nanoparticles (CPNPs) containing the NIR emitting fluorophore indocyanine green (ICG). These particles also possessed carboxylate and PEG surface functionality and were colloidally stable [165]. The quantum efficiency and photostability of the ICG-CPNPs were greater compared with the free dye. ICG-CPNPs injected intravenously in a nude mouse model showed significant accumulation in breast adenocarcinoma tumors (Figure 5B) [165].

3.3 Perfluorocarbon nanoparticles

Perfluorocarbon nanoparticles (PFCNPs), pioneered by Lanza, Wickline and others, have received considerable attention for their applications in molecular imaging and targeted drug delivery applications [169-172]. PFCNPs act as a platform to carry contrast-enhancing agents or chemotherapeutic drugs [170,172,173]. Functionalized PFCNPs are compatible with several molecular imaging modalities, including MRI and CT [170,172-174]. Typical PFCNPs contain a PFC core encapsulated in a lipid monolayer [171]. The PFC core has been shown to be a relatively non-volatile, inert, non-toxic and non-degradable material. Various biomolecules, including antibodies, peptides and peptidomimetics, can be covalently bound to the lipid layer for applications in molecular imaging [170-172]. Contrast enhancers such as gadolinium chelates can be covalently attached to the lipid layer. Functionalized PFCNP contrast agents have been used as molecular imaging agents in MRI assessments of tumor angiogenesis [175], cellular tracking [176,177] and atherosclerosis [178].

3.4 Lipid-based nanoparticles

Lipid-based nanoparticles such as liposomes and micelles have been developed for pharmaceuticals and aim to address the traditional boundaries to drug delivery [179-181]. Lipids are amphiphilic molecules containing both hydrophilic and hydrophobic portions that self-assemble in aqueous environments. Application of these particles as contrast agents for bioimaging is relatively new and very few studies have been performed [181]. Typically, the lipids act as a shell to enclose contrast enhancers such as iron oxide nanoparticles, perfluorocarbon nanoparticles or QDs [181]. Also, various targeting ligands or biomolecules can be covalently conjugated to enable selective accumulation of the particles [181]. Mulder *et al.* pioneered the use of lipid-based nanoparticles for contrast-enhanced MRI and molecular imaging applications [181]. Koole *et al.* recently developed paramagnetic lipid-coated silica nanoparticles containing a quantum dot core as a contrast agent for multimodal imaging (fluorescence and MRI) of $\alpha_v\beta_3$-integrin expression on cultured endothelial cells [182]. Also, Cressman *et al.* recently developed an RGD-labeled lipid incorporated into liposomal nanoparticles and studied trafficking in cultured endothelial cells [183]. Senarath-Yapa *et al.* furthered this work by reporting the use of poly(lipid)-coated, fluorophore-doped silica nanoparticles for biolabeling and cellular imaging applications [184].

4. Toxicity considerations

Owing to the rapid growth of nanoparticle use in biomedical research, the toxicity of these materials should be considered in detail [23,185,186]. Complete characterization of size [186], shape [187], charge [188,189], surface chemistry [189-191] and material properties is important when correlating toxicity. Nanomaterials may agglomerate *in vitro* or *in vivo* and may chemically degrade, making it difficult to relate systematically nanoparticle toxicity to such a diverse set of materials. Mechanisms of *in vitro* and *in vivo* toxicity have been reviewed thoroughly elsewhere [192]. Detailed studies of biodistribution, pharmacokinetics, and local and systemic toxicity, for each type of nanoparticle, will be important in overall toxicity evaluations. Although there is significant progress in the development of nanomaterials for biomedical applications, the study of nanotoxicology has thus far lagged behind [193]. There is a significant need for the development of rapid and efficient methods to identify the toxicity of nanomaterials, which is being addressed by initiatives such as the Nanotechnology Characterization Laboratory, NCI [194].

5. Summary and conclusions

Structural design of nanomaterials for biomedical imaging continues to expand and diversify. The size and surface characteristics of nanoparticles tend to determine their distribution, uptake and elimination. Nanoparticle sizes ranging between 10 and 100 nm or slightly larger are desired for use in molecular imaging applications. Significantly larger nanoparticles may undergo more rapid clearance via the RES whereas smaller particles may be cleared renally. The density and size of the targeting ligands on the nanoparticle surface also play an obvious role on the overall effectiveness of the contrast agent in molecular imaging. For reduced adsorption of serum components and extending circulation, PEG and other hydrophilic polymers are commonly used as surface modifiers. Although a multitude of functionalized nanoparticles have been synthesized so far, detailed *in vivo* toxicity studies have lagged behind.

This review summarizes emerging research on several of the more prominent types of nanoparticle-based contrast agent being investigated for biomedical imaging. Quantum dots are among the most promising agents for fluorescent imaging. The rich surface chemistry and absorption capacity of gold nanoparticles have triggered interest for their use in X-ray CT imaging applications. Engineered iron oxide nanoparticles with precise control over size and composition along with new nanoparticle–gadolinium conjugates are being explored as contrast agents for MRI. Although nanoparticle-based molecular imaging applications are moving towards clinical applications, formulation challenges such as aggregation and storage in clinical settings remain a challenge.

6. Expert opinion

In the past decade, advancements of nanotechnology in biomedical imaging have been greatly accelerated and have the promise of accurate molecular imaging with substantially improved contrast enhancement over conventional imaging agents. For example, multiple reports have identified tumors in animals at a much earlier stage when compared with clinical methods used today. As the field matures, developments in personalized medicine coupled with molecular targeting of therapeutics will continue. Although the current trends of nanoparticles in biomedical imaging appear promising, methods and models to measure and manipulate pharmacokinetics, biodistribution and toxicity will require more attention. First steps have been taken to formalize the characterization of nanomaterials used in bioimaging, and standardized methods, such as those provided by the Nanotechnology

Characterization Laboratory, offer an excellent benchmark for systematically studying nanomaterials for biological applications.

Design and development of carefully validated nanoparticle-based contrast agents for biomedical imaging requires a wide range of expertise ranging from chemistry and cell biology to engineering and radiology. Continuation of this multidisciplinary research approach will be required to actualize products. For example, nanoparticle-based contrast agents are being designed to be selective to receptors, which will require expertise in target identification, colloidal chemistry, biochemistry, analysis and stabilization. The formulation approach to develop a biomedical imaging agent may parallel the development of new therapeutic drugs; however, further challenges will emerge to address colloid stability and the stability of conjugated ligands. As nanoparticle contrast agents move into the clinic, challenges will emerge regarding reproducible large-scale production of these products that achieves a high value-to-cost ratio. In addition, researchers will have to be alert to potential problems such as occlusions, renal toxicity, hepatotoxicity, and so on, that may go unnoticed in early stage animal studies. For example, publications have a tendency to emphasize a fivefold increase in tumor specificity of a contrast agent without addressing the 10-fold increase in liver concentration. Rudimentary toxicity tests based on blood samples are generally quite simple and should be integrated into *in vivo* studies whenever possible.

Future use of nanoparticles in biomedical imaging appears promising. Synthesis strategies should continue to develop non-toxic, biocompatible and biodegradable nanoparticles that overcome nonspecific organ uptake and RES. To improve the likelihood of translation into the clinic, doses of nanoparticles could be lowered to accentuate imaging performance by increasing the contrast-to-noise ratio, by targeting the agent to tissues of interest, or by improving instrument sensitivity. Researchers working in this area should also consider any potential costs of implementing sophisticated imaging instrumentation and be attentive to the challenge of handling and interpreting large data sets obtained using nanoparticle contrast agents. As with any product for use in humans, extensive safety and toxicology studies will need to parallel pharmacokinetic and biodistribution studies in early stage clinical trials. Finally, emerging concepts using nanoparticles with multiple functions (e.g., imaging and therapeutic) should thoroughly consider the regulatory complexity of these types of combination approach.

Acknowledgments

Declaration of interest: The authors thank the Pacific Northwest National Laboratory for Laboratory Directed Research and Development Fund (operated by Battelle for the US Department of Energy under Contract DE-AC05-76RL01830), the American Heart Association, the NIH (R03 AR054035, P20 RR016443, R21 CA132033 and P20 RR015563), the NSF (CHE0719464) and the American Cancer Society (RSG-08-133-01-CDD).

Bibliography

1. Niemeyer CM. Nanoparticles, proteins, and nucleic acids: biotechnology meets materials science. Angew Chem Int Ed. 2001; 40(22):4128–58.
2. Ferrari M. Cancer nanotechnology: opportunities and challenges. Nat Rev Cancer. 2005; 5(3):161–71. [PubMed: 15738981]
3. Forrest ML, Kwon GS. Clinical developments in drug delivery nanotechnology. Adv Drug Deliv Rev. 2008; 60(8):861–2. [PubMed: 18358557]
4. Greish K. Enhanced permeability and retention of macromolecular drugs in solid tumors: A royal gate for targeted anticancer nanomedicines. J Drug Target. 2007; 15(7-8):457–64. [PubMed: 17671892]

5. Hawley AE, Illum L, Davis SS. Preparation of biodegradable, surface engineered PLGA nanospheres with enhanced lymphatic drainage and lymph node uptake. Pharm Res. 1997; 14(5): 657–61. [PubMed: 9165539]
6. Davis ME, Chen Z, Shin DM. Nanoparticle therapeutics: an emerging treatment modality for cancer. Nat Rev Drug Discov. 2008; 7(9):771–82. [PubMed: 18758474]
7. Weissleder R. Molecular imaging in cancer. Science. 2006; 312(5777):1168–71. [PubMed: 16728630]
8. Smith AM, Duan HW, Mohs AM, Nie SM. Bioconjugated quantum dots for in vivo molecular and cellular imaging. Adv Drug Deliv Rev. 2008; 60(11):1226–40. [PubMed: 18495291]
9. Lee S, Chen XY. Dual-modality probes for in vivo molecular imaging. Mol Imaging. 2009; 8(2):87–100. [PubMed: 19397854]
10. Prencipe G, Tabakman SM, Welsher K, Liu Z, et al. PEG branched polymer for functionalization of nanomaterials with ultralong blood circulation. J Am Chem Soc. 2009; 131(13):4783–87. [PubMed: 19173646]
11. Al-Jamal WT, Al-Jamal KT, Bomans PH, et al. Functionalized-quantum-dot-liposome hybrids as multimodal nanoparticles for cancer. Small. 2008; 4(9):1406–15. [PubMed: 18711753]
12. Yu SB, Watson AD. Metal-based X-ray contrast media. Chem Rev. 1999; 99(9):2353–77. [PubMed: 11749484]
13. Hainfeld JF, Slatkin DN, Focella TM, Smilowitz HM. Gold nanoparticles: a new X-ray contrast agent. Br J Radiol. 2006; 79(939):248–53. [PubMed: 16498039]
14. Choi HS, Liu W, Misra P, et al. Renal clearance of quantum dots. Nat Biotechnol. 2007; 25(10): 1165–70. [PubMed: 17891134]
15. Longmire M, Choyke PL, Kobayashi H. Clearance properties of nano-sized particles and molecules as imaging agents: considerations and caveats. Nanomedicine-UK. 2008; 3(5):703–17.
16. Popovtzer R, Agrawal A, Kotov NA, et al. Targeted gold nanoparticles enable molecular CT imaging of cancer. Nano Lett. 2008; 8(12):4593–6. [PubMed: 19367807]
17. McCarthy JR, Weissleder R. Multifunctional magnetic nanoparticles for targeted imaging and therapy. Adv Drug Deliv Rev. 2008; 60(11):1241–51. [PubMed: 18508157]
18. Weissleder R, Kelly K, Sun EY, et al. Cell-specific targeting of nanoparticles by multivalent attachment of small molecules. Nat Biotechnol. 2005; 23(11):1418–23. [PubMed: 16244656]
19. Byrne JD, Betancourt T, Brannon-Peppas L. Active targeting schemes for nanoparticle systems in cancer therapeutics. Adv Drug Deliv Rev. 2008; 60(15):1615–26. [PubMed: 18840489]
20. Cai WB, Chen XY. Nanoplatforms for targeted molecular imaging in living subjects. Small. 2007; 3(11):1840–54. [PubMed: 17943716]
21. Murphy CJ, Gole AM, Stone JW, et al. Gold Nanoparticles in biology: beyond toxicity to cellular imaging. Acc Chem Res. 2008; 41(12):1721–30. [PubMed: 18712884]
22. Sperling RA, Gil PR, Zhang F, et al. Biological applications of gold nanoparticles. Chem Soc Rev. 2008; 37(9):1896–908. [PubMed: 18762838]
23. Lewinski N, Colvin V, Drezek R. Cytotoxicity of nanoparticles. Small. 2008; 4(1):26–49. [PubMed: 18165959]
24. Daniel MC, Astruc D. Gold nanoparticles: assembly, supramolecular chemistry, quantum-size-related properties, and applications toward biology, catalysis, and nanotechnology. Chem Rev. 2004; 104(1):293–346. [PubMed: 14719978]
25. Turkevich J, Stevenson PC, Hillier J. A study of the nucleation and growth processes in the synthesis of colloidal gold. Discuss Faraday Soc. 1951; 11:55–75.
26. Kimling J, Maier M, Okenve B, et al. Turkevich method for gold nanoparticle synthesis revisited. J Phys Chem B. 2006; 110(32):15700–7. [PubMed: 16898714]
27. Brust M, Walker M, Bethell D, et al. Synthesis of thiol-derivatized gold nanoparticles in a 2-phase liquid-liquid system. J Chem Soc Chem Comm. 1994; 7(7):801–2.
28. Brust M, Fink J, Bethell D, et al. Synthesis and reactions of functionalized gold nanoparticles. J Chem Soc Chem Comm. 1995; 21(16):1655–6.
29. Pandey P, Singh SP, Arya SK, et al. Application of thiolated gold nanoparticles for the enhancement of glucose oxidase activity. Langmuir. 2007; 23(6):3333–7. [PubMed: 17261046]

30. Wangoo N, Bhasin KK, Mehta SK, Suri CR. Synthesis and capping of water-dispersed gold nanoparticles by an amino acid: bioconjugation and binding studies. J Colloid Interface Sci. 2008; 323(2):247–54. [PubMed: 18486946]

31. Wilson R. The use of gold nanoparticles in diagnostics and detection. Chem Soc Rev. 2008; 37(9): 2028–45. [PubMed: 18762845]

32. Blaszkiewicz P. Synthesis of water-soluble ionic and nonionic iodinated X-Ray contrast-media. Invest Radiol. 1994; 29:S51–3. [PubMed: 8071045]

33. Galperin A, Margel D, Baniel J, et al. Radiopaque iodinated polymeric nanoparticles for X-ray imaging applications. Biomaterials. 2007; 28(30):4461–8. [PubMed: 17644171]

34. Kattumuri V, Katti K, Bhaskaran S, et al. Gum arabic as a phytochemical construct for the stabilization of gold nanoparticles: in vivo pharmacokinetics and X-ray-contrast-imaging studies. Small. 2007; 3(2):333–41. [PubMed: 17262759]

35. Kim D, Park S, Lee JH, et al. Antibiofouling polymer-coated gold nanoparticles as a contrast agent for in vivo X-ray computed tomography imaging. J Am Chem Soc. 2007; 129:7661–65. [PubMed: 17530850]

36. Nikoobakht B, El-Sayed MA. Preparation and growth mechanism of gold nanorods (NRs) using seed-mediated growth method. Chem Mater. 2003; 15(10):1957–62.

37. Zhao W, Brook MA, Li YF. Design of gold nanoparticle-based colorimetric biosensing assays. Chembiochem. 2008; 9(15):2363–71. [PubMed: 18821551]

38. Elghanian R, Storhoff JJ, Mucic RC, et al. Selective colorimetric detection of polynucleotides based on the distance-dependent optical properties of gold nanoparticles. Science. 1997; 277(5329):1078–81. [PubMed: 9262471]

39. Mirkin CA. Programming the assembly of two- and three-dimensional architectures with DNA and nanoscale inorganic building blocks. Inorg Chem. 2000; 39(11):2258–72. [PubMed: 12526483]

40. Liu JW, Lu Y. Accelerated color change of gold nanoparticles assembled by DNAzymes for simple and fast colorimetric Pb2+ detection. J Am Chem Soc. 2004; 126(39):12298–305. [PubMed: 15453763]

41. Li HQ, Wang CG, Ma ZF, Su ZM. Colorimetric detection of immunoglobulin G by use of functionalized gold nanoparticles on polyethylenimine film. Anal Bioanal Chem. 2006; 384(7-8): 1518–24. [PubMed: 16534577]

42. Lee JS, Han MS, Mirkin CA. Colorimetric detection of mercuric ion (Hg2+) in aqueous media using DNA-functionalized gold nanoparticles. Angew Chem Int Ed. 2007; 46(22):4093–6.

43. Lee JS, Ulmann PA, Han MS, Mirkin CA. A DNA-gold nanoparticle-based colorimetric competition assay for the detection of cysteine. Nano Lett. 2008; 8(2):529–33. [PubMed: 18205426]

44. Gao XH, Cui YY, Levenson RM, et al. In vivo cancer targeting and imaging with semiconductor quantum dots. Nat Biotechnol. 2004; 22(8):969–76. [PubMed: 15258594]

45. Resch-Genger U, Grabolle M, Cavaliere-Jaricot S, et al. Quantum dots versus organic dyes as fluorescent labels. Nat Methods. 2008; 5(9):763–75. [PubMed: 18756197]

46. Zhang H, Yee D, Wang C. Quantum dots for cancer diagnosis and therapy: biological and clinical perspectives. Nanomedicine-UK. 2008; 3(1):83–91.

47. Misra RD. Quantum dots for tumor-targeted drug delivery and cell imaging. Nanomedicine-UK. 2008; 3(3):271–4.

48. Ekimov AI, Onushchenko AA. Quantum size effect in the optical-spectra of semiconductor micro-crystals. Sov Phys Semicond+. 1982; 16(7):775–8.

49. Efros AL, Efros AL. Interband absorption of light in a semiconductor sphere. Sov Phys Semicond +. 1982; 16(7):772–5.

50. Murray CB, Norris DJ, Bawendi MG. Synthesis and characterization of nearly monodisperse Cde (E = S, Se, Te) semiconductor nanocrystallites. J Am Chem Soc. 1993; 115(19):8706–15.

51. Hines MA, Guyot-Sionnest P. Synthesis and characterization of strongly luminescing ZnS-Capped CdSe nanocrystals. J Phys Chem-US. 1996; 100(2):468–71.

52. Gerion D, Pinaud F, Williams SC, et al. Synthesis and properties of biocompatible water-soluble silica-coated CdSe/ZnS semiconductor quantum dots. J Phys Chem B. 2001; 105(37):8861–71.

53. Talapin DV, Mekis I, Gotzinger S, et al. CdSe/CdS/ZnS and CdSe/ZnSe/ZnS core-shell-shell nanocrystals. J Phys Chem B. 2004; 108(49):18826–31.
54. Joshi A, Narsingi KY, Manasreh MO, et al. Temperature dependence of the band gap of colloidal CdSe/ZnS core/shell nanocrystals embedded into an ultraviolet curable resin. Appl Phys Lett. 2006; 89(13):131907.
55. Dabbousi BO, Rodriguezviejo J, Mikulec FV, et al. (CdSe)ZnS core-shell quantum dots: Synthesis and characterization of a size series of highly luminescent nanocrystallites. J Phys Chem B. 1997; 101(46):9463–75.
56. Roy MD, Herzing AA, Lacerda SHDP, Becker ML. Emission-tunable microwave synthesis of highly luminescent water soluble CdSe/ZnS quantum dots. Chem Commun. 2008; 14(18):2106–8.
57. Deng ZT, Lie FL, Shen SY, et al. Water-based route to ligand-selective synthesis of ZnSe and Cd-doped ZnSe quantum dots with tunable ultraviolet A to blue photoluminescence. Langmuir. 2009; 25(1):434–42. [PubMed: 19053829]
58. Bruchez M, Moronne M, Gin P, et al. Semiconductor nanocrystals as fluorescent biological labels. Science. 1998; 281(5385):2013–6. [PubMed: 9748157]
59. Xu J, Wang J, Mitchell M, et al. Organic-inorganic nanocomposites via directly grafting conjugated polymers onto quantum dots. J Am Chem Soc. 2007; 129(42):12828–33. [PubMed: 17914821]
60. Anderson RE, Chan WCW. Systematic investigation of preparing biocompatible, single, and small ZnS-capped CdSe quantum dots with amphiphilic polymers. ACS Nano. 2008; 2(7):1341–52. [PubMed: 19206301]
61. Bentzen EL, Tomlinson ID, Mason J, et al. Surface modification to reduce nonspecific binding of quantum dots in live cell assays. Bioconjug Chem. 2005; 16(6):1488–94. [PubMed: 16287246]
62. Xing Y, Chaudry Q, Shen C, et al. Bioconjugated quantum dots for multiplexed and quantitative immunohistochemistry. Nat Protoc. 2007; 2(5):1152–65. [PubMed: 17546006]
63. Pathak S, Davidson MC, Silva GA. Characterization of the functional binding properties of antibody conjugated quantum dots. Nano Lett. 2007; 7(7):1839–45. [PubMed: 17536868]
64. Qian J, Yong KT, Roy I, et al. Imaging pancreatic cancer using surface-functionalized quantum dots. J Phys Chem B. 2007; 111(25):6969–72. [PubMed: 17552555]
65. Wamement MR, Tomlinson ID, Chang JC, et al. Controlling the reactivity of ampiphilic quantum dots in biological assays through hydrophobic assembly of custom PEG derivatives. Bioconjug Chem. 2008; 19(7):1404–13. [PubMed: 18529022]
66. Akerman ME, Chan WCW, Laakkonen P, et al. Nanocrystal targeting in vivo. Proc Natl Acad Sci USA. 2002; 99(20):12617–21. [PubMed: 12235356]
67. Cai WB, Shin DW, Chen K, et al. Peptide-labeled near-infrared quantum dots for imaging tumor vasculature in living subjects. Nano Lett. 2006; 6(4):669–76. [PubMed: 16608262]
68. Ballou B, Lagerholm BC, Ernst LA, et al. Noninvasive imaging of quantum dots in mice. Bioconjug Chem. 2004; 15(1):79–86. [PubMed: 14733586]
69. Kim S, Fisher B, Eisler HY, Bawendi MG. Novel type-II quantum dots: CDTE/CDSE(core/shell) and CDSE/ZNTE (core/shell) heterostructures. J Am Chem Soc. 2003; 125(38):11466–67. [PubMed: 13129327]
70. Kim S, Lim YT, Soltesz EG, et al. Near-infrared fluorescent type II quantum dots for sentinel lymph node mapping. Nat Biotechnol. 2004; 22(1):93–7. [PubMed: 14661026]
71. Tada H, Higuchi H, Wanatabe TM, Ohuchi N. In vivo real-time tracking of single quantum dots conjugated with monoclonal anti-HER2 antibody in tumors of mice. Cancer Res. 2007; 67(3): 1138–44. [PubMed: 17283148]
72. Gao XL, Chen J, Chen JY, et al. Quantum dots bearing lectin-functionalized nanoparticles as a platform for in vivo brain imaging. Bioconjug Chem. 2008; 19(11):2189–95. [PubMed: 18922029]
73. Yong KT. Mn-doped near-infrared quantum dots as multimodal targeted probes for pancreatic cancer imaging. Nanotechnology. 2009; 20(1):015102. [PubMed: 19417242]
74. Jin T, Yoshioka Y, Fujii F, et al. Gd3+-functionalized near-infrared quantum dots for in vivo dual modal (fluorescence/magnetic resonance) imaging. Chem Commun. 2008; 44:5764–6.

75. Thorek DLJ, Tsourkas A. Size, charge and concentration dependent uptake of iron oxide particles by non-phagocytic cells. Biomaterials. 2008; 29(26):3583–90. [PubMed: 18533252]
76. Shi XY, Wang SH, Swanson SD, et al. Dendrimer-functionalized shell-crosslinked iron oxide nanoparticles for in-vivo magnetic resonance imaging of tumors. Adv Mater. 2008; 20(9):1671–78.
77. Peng XH, Qian XM, Mao H, et al. Targeted magnetic iron oxide nanoparticles for tumor imaging and therapy. Int J Nanomed. 2008; 3(3):311–21.
78. Hwu YSL Jr, Josephrajan T, Hsu MH, et al. Shieh targeted paclitaxel by conjugation to iron oxide and gold nanoparticles. J Am Chem Soc. 2009; 131(1):66–8. [PubMed: 19072111]
79. Jarrett BR, Frendo M, Vogan J, Louie AY. Size-controlled synthesis of dextran sulfate coated iron oxide nanoparticles for magnetic resonance imaging. Nanotechnology. 2007; 18(3):35603.
80. Sun C, Lee JSH, Zhang MQ. Magnetic nanoparticles in MR imaging and drug delivery. Adv Drug Deliv Rev. 2008; 60(11):1252–65. [PubMed: 18558452]
81. Neumaier CE, Baio G, Ferrini S, et al. MR and iron magnetic nanoparticles. Imaging opportunities in preclinical and translational research. Tumori. 2008; 94(2):226–33. [PubMed: 18564611]
82. Jun YW, Lee JH, Cheon J. Chemical design of nanoparticle probes for high-performance magnetic resonance imaging. Angew Chem Int Ed. 2008; 47(28):5122–35.
83. Schulze E, Ferrucci JT, Poss K, et al. Cellular uptake and trafficking of a prototypical magnetic iron-oxide label in-vitro. Invest Radiol. 1995; 30(10):604–10. [PubMed: 8557500]
84. Saini S, Stark DD, Hahn PF, et al. Ferrite particles - a superparamagnetic Mr contrast agent for the reticuloendothelial system. Radiology. 1987; 162(1):211–6. [PubMed: 3786765]
85. Gandon Y, Brunet F, Guyader D, et al. Superparamagnetic iron-oxide (Sio) - an Mr imaging contrast-medium for the reticuloendothelial system. Ann Radiol. 1989; 32(4):267–72. [PubMed: 2554776]
86. Wunderbaldinger P, Josephson L, Weissleder R. Crosslinked iron oxides (CLIO): a new platform for the development of targeted MR contrast agents. Acad Radiol. 2002; 9:S304–6. [PubMed: 12188255]
87. Mergo PJ, Engelken JD, Helmberger T, Ros PR. MRI in focal liver disease: a comparison of small and ultra-small superparamagnetic iron oxide as hepatic contrast agents. J Magn Reson Imaging. 1998; 8(5):1073–8. [PubMed: 9786144]
88. Kawahara I, Nakamoto M, Kitagawa N, et al. Potential of magnetic resonance plaque imaging using superparamagnetic particles of iron oxide for the detection of carotid plaque. Neurol Med Chir. 2008; 48(4):157–62.
89. Feltin N, Pileni MP. New technique for synthesizing iron ferrite magnetic nanosized particles. Langmuir. 1997; 13(15):3927–33.
90. Prakash A, McCormick AV, Zachariah MR. Aero-sol-gel synthesis of nanoporous iron-oxide particles: a potential oxidizer for nanoenergetic materials. Chem Mater. 2004; 16(8):1466–71.
91. Srivastava DN, Perkas N, Gedanken A, Felner I. Sonochemical synthesis of mesoporous iron oxide and accounts of its magnetic and catalytic properties. J Phys Chem B. 2002; 106(8):1878–83.
92. Bautista MC, Bomati-Miguel O, Morales MD, et al. Surface characterisation of dextran-coated iron oxide nanoparticles prepared by laser pyrolysis and coprecipitation. J Magn Magn Mater. 2005; 293(1):20–7.
93. Hua CC, Zakaria S, Farahiyan R, et al. Size-controlled synthesis and characterization of Fe3O4 nanoparticles by chemical coprecipitation method. Sains Malays. 2008; 37(4):389–94.
94. Fauconnier N, Pons JN, Roger J, Bee A. Thiolation of maghemite nanoparticles by dimercaptosuccinic acid. J Colloid Interface Sci. 1997; 194(2):427–33. [PubMed: 9398425]
95. Mohammadi Z, Cole A, Berkland CJ. In situ synthesis of iron oxide within polyvinylamine nanoparticle reactors. J Phys Chem C. 2009; 113(18):7652–8.
96. Jun YW, Huh YM, Choi JS, et al. Nanoscale size effect of magnetic nanocrystals and their utilization for cancer diagnosis via magnetic resonance imaging. J Am Chem Soc. 2005; 127(16): 5732–3. [PubMed: 15839639]
97. Sun SH, Zeng H, Robinson DB, et al. Monodisperse MFe2O4 (M = Fe, Co, Mn) nanoparticles. J Am Chem Soc. 2004; 126(1):273–9. [PubMed: 14709092]

98. Lee JH, Huh YM, Jun Y, et al. Artificially engineered magnetic nanoparticles for ultra-sensitive molecular imaging. Nat Med. 2007; 13(1):95–9. [PubMed: 17187073]

99. Di Marco M, Guilbert I, Port M, et al. Colloidal stability of ultrasmall superparamagnetic iron oxide (USPIO) particles with different coatings. Int J Pharm. 2007; 331(2):197–203. [PubMed: 17141984]

100. Park JY, Daksha P, Lee GH, et al. Highly water-dispersible PEG surface modified ultra small superparamagnetic iron oxide nanoparticles useful for target-specific biomedical applications. Nanotechnology. 2008; 19(36):365603.

101. Peng S, Wang C, Xie J, Sun SH. Synthesis and stabilization of monodisperse Fe nanoparticles. J Am Chem Soc. 2006; 128(33):10676–7. [PubMed: 16910651]

102. Kohler N, Fryxell GE, Zhang MQ. A bifunctional poly(ethylene glycol) silane immobilized on metallic oxide-based nanoparticles for conjugation with cell targeting agents. J Am Chem Soc. 2004; 126(23):7206–11. [PubMed: 15186157]

103. Sun EY, Josephson L, Kelly KA, Weissleder R. Development of nanoparticle libraries for biosensing. Bioconjug Chem. 2006; 17(1):109–13. [PubMed: 16417258]

104. Waters EA, Wickline SA. Contrast agents for MRI. Basic Res Cardiol. 2008; 103(2):114–21. [PubMed: 18324367]

105. Weissleder R, Imhof H. Molecular imaging - a new focal point of radiology. Radiologe. 2007; 47(1):6–7. [PubMed: 17136404]

106. Wunderbaldinger P, Josephson L, Bremer C, et al. Detection of lymph node metastases by contrast-enhanced MRI in an experimental model. Magn Reson Med. 2002; 47(2):292–7. [PubMed: 11810672]

107. Lewin M, Carlesso N, Tung CH, et al. Tat peptide-derivatized magnetic nanoparticles allow in vivo tracking and recovery of progenitor cells. Nat Biotechnol. 2000; 18(4):410–4. [PubMed: 10748521]

108. Kircher MF, Allport JR, Graves EE, et al. In vivo high resolution three-dimensional imaging of antigen-specific cytotoxic T-lymphocyte trafficking to tumors. Cancer Res. 2003; 63(20):6838–46. [PubMed: 14583481]

109. Kircher MF, Mahmood U, King RS, et al. A multimodal nanoparticle for preoperative magnetic resonance imaging and intraoperative optical brain tumor delineation. Cancer Res. 2003; 63(23): 8122–5. [PubMed: 14678964]

110. Montet X, Weissleder R, Josephson L. Imaging pancreatic cancer with a peptide-nanoparticle conjugate targeted to normal pancreas. Bioconjug Chem. 2006; 17(4):905–11. [PubMed: 16848396]

111. Schellenberger EA, Hogemann D, Josephson L, Weissleder R. Annexin V-CLIO: a nanoparticle for detecting apoptosis by MRI. Acad Radiol. 2002; 9:S310–1. [PubMed: 12188257]

112. Hu FQ, Wei L, Zhou Z, et al. Preparation of biocompatible magnetite nanocrystals for in vivo magnetic resonance detection of cancer. Adv Mater. 2006; 18(19):2553–56.

113. Song HT, Choi JS, Huh YM, et al. Surface modulation of magnetic nanocrystals in the development of highly efficient magnetic resonance probes for intracellular labeling. J Am Chem Soc. 2005; 127(28):9992–3. [PubMed: 16011350]

114. Miyoshi S, Flexman JA, Cross DJ, et al. Transfection of neuroprogenitor cells with iron nanoparticles for magnetic resonance imaging tracking: Cell viability, differentiation, and intracellular localization. Mol Imaging Biol. 2005; 7(4):286–95. [PubMed: 16080022]

115. Xie J, Chen K, Lee HY, et al. Ultrasmall c(RGDyK)-coated Fe3O4 nanoparticles and their specific targeting to integrin alpha(v)beta(3)-rich tumor cells. J Am Chem Soc. 2008; 130(24): 7542–43. [PubMed: 18500805]

116. Huh YM, Jun YW, Song HT, et al. In vivo magnetic resonance detection of cancer by using multifunctional magnetic nanocrystals. J Am Chem Soc. 2005; 127(35):12387–91. [PubMed: 16131220]

117. Iijima S. Helical microtubules of graphitic carbon. Nature. 1991; 354(6348):56–8.

118. Bachilo SM, Strano MS, Kittrell C, et al. Structure-assigned optical spectra of single-walled carbon nanotubes. Science. 2002; 298(5602):2361–6. [PubMed: 12459549]

119. Kam NWS, Jessop TC, Wender PA, Dai HJ. Nanotube molecular transporters: internalization of carbon nanotube-protein conjugates into mammalian cells. J Am Chem Soc. 2004; 126(22): 6850–1. [PubMed: 15174838]
120. Pantarotto D, Briand JP, Prato M, Bianco A. Translocation of bioactive peptides across cell membranes by carbon nanotubes. Chem Commun. 2004; 7(1):16–7.
121. Dai HJ, Hafner JH, Rinzler AG, et al. Nanotubes as nanoprobes in scanning probe microscopy. Nature. 1996; 384(6605):147–50.
122. Lacerda L, Soundararajan A, Singh R, et al. Dynamic imaging of functionalized multi-walled carbon nanotube systemic circulation and urinary excretion. Adv Mater. 2008; 20(2):225–30.
123. Guo T, Nikolaev P, Thess A, et al. Catalytic growth of single-walled nanotubes by laser vaporization. Chem Phys Lett. 1995; 243(1-2):49–54.
124. Hafner JH, Bronikowski MJ, Azamian BR, et al. Catalytic growth of single-wall carbon nanotubes from metal particles. Chem Phys Lett. 1998; 296(1-2):195–202.
125. Treacy MMJ, Ebbesen TW, Gibson JM. Exceptionally high Young's modulus observed for individual carbon nanotubes. Nature. 1996; 381(6584):678–80.
126. Bianco A, Kostarelos K, Partidos CD, Prato M. Biomedical applications of functionalised carbon nanotubes. Chem Commun. 2005; 5:571–7.
127. Sirdeshmukh, R.; Teker, K.; Panchapakesan, B. Functionalization of carbon nanotubes with antibodies for breast cancer detection applications. Proceedings of the 2004 International Conference on MEMS, NANO, and Smart Systems; 2004. p. 48-53.
128. Cherukuri P, Bachilo SM, Litovsky SH, Weisman RB. Near-infrared fluorescence microscopy of single-walled carbon nanotubes in phagocytic cells. J Am Chem Soc. 2004; 126(48):15638–9. [PubMed: 15571374]
129. Svenson S, Tomalia DA. Commentary - dendrimers in biomedical applications - reflections on the field. Adv Drug Deliv Rev. 2005; 57(15):2106–29. [PubMed: 16305813]
130. Kobayashi H, Brechbiel MW. Nano-sized MRI contrast agents with dendrimer cores. Adv Drug Deliv Rev. 2005; 57(15):2271–86. [PubMed: 16290152]
131. Tomalia DA, Reyna LA, Svenson S. Dendrimers as multi-purpose nanodevices for oncology drug delivery and diagnostic imaging. Biochem Soc T. 2007; 35:61–7.
132. Langereis S, Dirksen A, Hackeng TM, et al. Dendrimers and magnetic resonance imaging. New J Chem. 2007; 31(7):1152–60.
133. Langereis S, de Lussanet QG, van Genderen MHP, et al. Evaluation of Gd(III)DTPA-terminated poly(propylene imine) dendrimers as contrast agents for MR imaging. NMR Biomed. 2006; 19(1):133–41. [PubMed: 16450331]
134. Tomalia DA. Starburst(R) dendrimers - nanoscopic supermolecules according dendritic rules and principles. Macromol Symp. 1996; 101:243–55.
135. Hawker CJ, Frechet JMJ. Preparation of polymers with controlled molecular architecture - a new convergent approach to dendritic macromolecules. J Am Chem Soc. 1990; 112(21):7638–47.
136. Tomalia DA. Birth of a new macromolecular architecture: dendrimers as quantized building blocks for nanoscale synthetic organic chemistry. Aldrichim Acta. 2004; 37(2):39–57.
137. Wiener EC, Brechbiel MW, Brothers H, et al. Dendrimer-based metal-chelates - a new class of magnetic-resonance-imaging contrast agents. Magn Reson Med. 1994; 31(1):1–8. [PubMed: 8121264]
138. Bryant LH, Brechbiel MW, Wu CC, et al. Synthesis and relaxometry of high-generation (G = 5, 7, 9, and 10) PAMAM dendrimer-DOTA-gadolinium chelates. J Magn Reson Imaging. 1999; 9(2):348–52. [PubMed: 10077036]
139. Kobayashi H, Kawamoto S, Jo SK, et al. Macromolecular MRI contrast agents with small dendrimers: pharmacokinetic differences between sizes and cores. Bioconjug Chem. 2003; 14(2): 388–94. [PubMed: 12643749]
140. Konda SD, Aref M, Brechbiel M, Wiener EC. Development of a tumor-targeting MR contrast agent using the high-affinity folate receptor - work in progress. Invest Radiol. 2000; 35(1):50–7. [PubMed: 10639036]

141. Konda SD, Wang S, Brechbiel M, Wiener EC. Biodistribution of a Gd-153-folate dendrimer, generation=4, in mice with folate-receptor positive and negative ovarian tumor xenografts. Invest Radiol. 2002; 37(4):199–204. [PubMed: 11923642]
142. Wiener EC, Konda SD, Wang S, Brechbiel M. Imaging folate binding protein expression with MRI. Acad Radiol. 2002; 9:S316–9. [PubMed: 12188260]
143. Wu CC, Brechbiel MW, Kozak RW, Gansow OA. Metal-chelate-dendrimer-antibody constructs for use in radioimmunotherapy and imaging. Bioorg Med Chem Lett. 1994; 4(3):449–54.
144. van Baal I, Malda H, Synowsky SA, et al. Multivalent peptide and protein dendrimers using native chemical ligation. Angew Chem Int Ed. 2005; 44(32):5052–7.
145. Konda SD, Aref M, Wang S, et al. Specific targeting of folate-dendrimer MRI contrast agents to the high affinity fo late receptor expressed in ovarian tumor xenografts. Magn Reson Mater Phy. 2001; 12(2-3):104–13.
146. Swanson SD, Kukowska-Latallo JF, Patri AK, et al. Targeted gadolinium-loaded dendrimer nanoparticles for tumor-specific magnetic resonance contrast enhancement. Int J Nanomed. 2008; 3(2):201–10.
147. De Geest BG, Sanders NN, Sukhorukov GB, et al. Release mechanisms for polyelectrolyte capsules. Chem Soc Rev. 2007; 36(4):636–49. [PubMed: 17387411]
148. Hartig SM, Greene RR, Dikov MM, et al. Multifunctional nanoparticulate polyelectrolyte complexes. Pharm Res. 2007; 24(12):2353–69. [PubMed: 17932727]
149. Liu ZH, Jiao YP, Wang YF, et al. Polysaccharides-based nanoparticles as drug delivery systems. Adv Drug Deliv Rev. 2008; 60(15):1650–62. [PubMed: 18848591]
150. de Vasconcelos CL, Bezerril PM, dos Santos DES, et al. Effect of molecular weight and ionic strength on the formation of polyelectrolyte complexes based on poly(methacrylic acid) and chitosan. Biomacromolecules. 2006; 7(4):1245–52. [PubMed: 16602745]
151. Hartig SM, Carlesso G, Davidson JM, Prokop A. Development of improved nanoparticulate polyelectrolyte complex physicochemistry by nonstoichiometric mixing of polyions with similar molecular weights. Biomacromolecules. 2007; 8(1):265–72. [PubMed: 17206816]
152. Decher G. Fuzzy nanoassemblies: toward layered polymeric multicomposites. Science. 1997; 277(5330):1232–7.
153. Hartig SM, Greene RR, Carlesso G, et al. Kinetic analysis of nanoparticulate polyelectrolyte complex interactions with endothelial cells. Biomaterials. 2007; 28(26):3843–55. [PubMed: 17560645]
154. Tiyaboonchai W, Woiszwillo J, Middaugh CR. Formulation and characterization of amphotericin B-polyethylenimine-dextran sulfate nanoparticles. J Pharm Sci-US. 2001; 90(7):902–14.
155. Tiyaboonchai W, Woiszwillo J, Sims RC, Middaugh CR. Insulin containing polyethylenimine-dextran sulfate nanoparticles. Int J Pharm. 2003; 255(1-2):139–51. [PubMed: 12672610]
156. Bailey MM, Berkland CJ. Nanoparticle formulations in pulmonary drug delivery. Med Res Rev. 2009; 29(1):196–212. [PubMed: 18958847]
157. Zaitsev S, Cartier R, Vyborov O, et al. Polyelectrolyte nanoparticles mediate vascular gene delivery. Pharm Res. 2004; 21(9):1656–61. [PubMed: 15497693]
158. Ii'ina AV, Varlamov VP. Chitosan-based polyelectrolyte complexes: a review. Appl Biochem Micro+. 2005; 41(1):5–11.
159. Huang M, Vitharana SN, Peek LJ, et al. Polyelectrolyte complexes stabilize and controllably release vascular endothelial growth factor. Biomacromolecules. 2007; 8(5):1607–14. [PubMed: 17428030]
160. Huang M, Huang ZL, Bilgen M, Berkland C. Magnetic resonance imaging of contrast-enhanced polyelectrolyte complexes. Nanomed Nanotechnol Biol Med. 2008; 4:30–40.
161. Liu T, Tang A, Zhang GY, et al. Calcium phosphate nanoparticles as a novel nonviral vector for efficient trasfection of DNA in cancer gene therapy. Cancer Biother Radiopharm. 2005; 20(2): 141–9. [PubMed: 15869447]
162. Maitra A. Calcium phosphate nanoparticles: second-generation nonviral vectors in gene therapy. Expert Rev Mol Diagn. 2005; 5(6):893–905. [PubMed: 16255631]

163. Morgan TT, Muddana HS, Altinoglu EI, et al. Encapsulation of organic molecules in calcium phosphate nanocomposite particles for intracellular imaging and drug delivery. Nano Lett. 2008; 8(12):4108–15. [PubMed: 19367837]
164. Kester M, Heakal Y, Fox T, et al. Calcium phosphate nanocomposite particles for in vitro imaging and encapsulated chemotherapeutic drug delivery to cancer cells. Nano Lett. 2008; 8(12):4116–21. [PubMed: 19367878]
165. Altinoglu EI, Russin TJ, Kaiser JM, et al. Near-infrared emitting fluorophore-doped calcium phosphate nanoparticles for in vivo imaging of human breast cancer. ACS Nano. 2008; 2(10): 2075–84. [PubMed: 19206454]
166. Roy I, Mitra S, Maitra A, Mozumdar S. Calcium phosphate nanoparticles as novel non-viral vectors for targeted gene delivery. Int J Pharm. 2003; 250(1):25–33. [PubMed: 12480270]
167. Bisht S, Bhakta G, Mitra S, Maitra A. pDNA loaded calcium phosphate nanoparticles: highly efficient non-viral vector for gene delivery. Int J Pharm. 2005; 288(1):157–68. [PubMed: 15607268]
168. Sokolova V, Kovtun A, Heumann R, Epple M. Tracking the pathway of calcium phosphate/DNA nanoparticles during cell transfection by incorporation of red-fluorescing tetramethylrhodamine isothiocyanate-bovine serum albumin into these nanoparticles. J Biol Inorg Chem. 2007; 12(2): 174–9. [PubMed: 17031704]
169. Lanza GM, Winter PM, Caruthers SD, et al. Nanomedicine opportunities for cardiovascular disease with perfluorocarbon nanoparticles. Nanomedicine-UK. 2006; 1(3):321–9.
170. Tran TD, Caruthers SD, Hughes M, et al. Clinical applications of perfluorocarbon nanoparticles for molecular imaging and targeted therapeutics. Int J Nanomed. 2007; 2(4):515–26.
171. Winter PM, Cai K, Caruthers SD, et al. Emerging nanomedicine opportunities with perfluorocarbon nanoparticles. Expert Rev Med Devices. 2007; 4(2):137–45. [PubMed: 17359221]
172. Hughes M, Caruthers S, Tran T, et al. Perfluorocarbon nanoparticles for molecular imaging and targeted therapeutics. P IEEE. 2008; 96(3):397–415.
173. Marsh JN, Partlow KC, Abendschein DR, et al. Molecular imaging with targeted perfluorocarbon nanoparticles: quantification of the concentration dependence of contrast enhancement for binding to sparse cellular epitopes. Ultrasound Med Biol. 2007; 33(6):950–8. [PubMed: 17434667]
174. Caruthers SD, Winter PM, Wickline SA, Lanza GM. Targeted magnetic resonance imaging contrast agents. Methods Mol Med. 2006; 124:387–400. [PubMed: 16506431]
175. Schmieder AH, Winter PM, Caruthers SD, et al. Molecular MR imaging of melanoma angiogenesis with alpha(nu)beta(3)-targeted paramagnetic nanoparticles. Magnet Reson Med. 2005; 53(3):621–7.
176. Ahrens ET, Flores R, Xu HY, Morel PA. In vivo imaging platform for tracking immunotherapeutic cells. Nat Biotechnol. 2005; 23(8):983–7. [PubMed: 16041364]
177. Partlow KC, Chen JJ, Brant JA, et al. F-19 magnetic resonance imaging for stem/progenitor cell tracking with multiple unique perfluorocarbon nanobeacons. FASEB J. 2007; 21(8):1647–54. [PubMed: 17284484]
178. Wickline SA, Neubauer AM, Winter PM, et al. Molecular imaging and therapy of atherosclerosis with targeted nanoparticles. J Magn Reson Imaging. 2007; 25(4):667–80. [PubMed: 17347992]
179. Muchow M, Maincent P, Muller RH. Lipid nanoparticles with a solid matrix (SLN, NLC, LDC) for oral drug delivery. Drug Dev Ind Pharm. 2008; 34(12):1394–405. [PubMed: 18665980]
180. Li XW, Sun LX, Lin XH, Zheng LQ. Solid lipid nanoparticles as drug delivery system. Prog Chem. 2007; 19(1):87–92.
181. Mulder WJM, Strijkers GJ, van Tilborg GAF, et al. Lipid-based nanoparticles for contrast-enhanced MRI and molecular imaging. NMR Biomed. 2006; 19(1):142–64. [PubMed: 16450332]
182. Koole R, van Schooneveld MM, Hilhorst J, et al. Paramagnetic lipid-coated silica nanoparticles with a fluorescent quantum dot core: a new contrast agent platform for multimodality imaging. Bioconjug Chem. 2008; 19(12):2471–9. [PubMed: 19035793]

183. Cressman S, Dobson I, Lee JB, Tam Y, et al. Synthesis of a labeled RGD–lipid, its incorporation into liposomal nanoparticles, and their trafficking in cultured endothelial Cells. Bioconjug Chem. 2009; 20(7):1404–11. [PubMed: 19534457]

184. Senarath-Yapa MD, Phimphivong S, Coym JW, et al. Preparation and characterization of poly(lipid)-coated, fluorophore-doped silica nanoparticles for biolabeling and cellular imaging. Langmuir. 2007; 23(25):12624–33. [PubMed: 17975939]

185. Lanone S, Boczkowski J. Biomedical applications and potential health risks of nanomaterials: molecular mechanisms. Curr Mol Med. 2006; 6(6):651–63. [PubMed: 17022735]

186. Pan Y, Neuss S, Leifert A, et al. Size-dependent cytotoxicity of gold nanoparticles. Small. 2007; 3(11):1941–9. [PubMed: 17963284]

187. Powers KW, Palazuelos M, Moudgil BM, Roberts SM. Characterization of the size, shape, and state of dispersion of nanoparticles for toxicological studies. Nanotoxicology. 2007; 1(1):42–51.

188. Simon A, Thiebault C, Reynaud C, et al. Toxicity of oxide nanoparticles and carbon nanotubes on cultured pneumocytes: impact of size, structure and surface charge. Toxicol Lett. 2006; 164:S222–S222.

189. Jiang JK, Oberdorster G, Biswas P. Characterization of size, surface charge, and agglomeration state of nanoparticle dispersions for toxicological studies. J Nanopart Res. 2009; 11(1):77–89.

190. Dobrovolskaia MA, Mcneil SE. Immunological properties of engineered nanomaterials. Nat Nanotechnol. 2007; 2(8):469–78. [PubMed: 18654343]

191. Clift MJD, Rothen-Rutishauser B, Brown DM, et al. The impact of different nanoparticle surface chemistry and size on uptake and toxicity in a murine macrophage cell line. Toxicol Appl Pharm. 2008; 232(3):418–27.

192. Aillon KL, Xie Y, El-Gendy N, et al. Effects of nanomaterial physicochemical properties on in vivo toxicity. Adv Drug Deliv Rev. 2009; 61(6):457–66. [PubMed: 19386275]

193. Fischer HC, Chan WCW. Nanotoxicity: the growing need for in vivo study. Curr Opin Biotech. 2007; 18(6):565–71. [PubMed: 18160274]

194. NCI.Nanotechnology Characterization Laboratory. Available from: http://nclcancergov/working_assay-cascadeasp

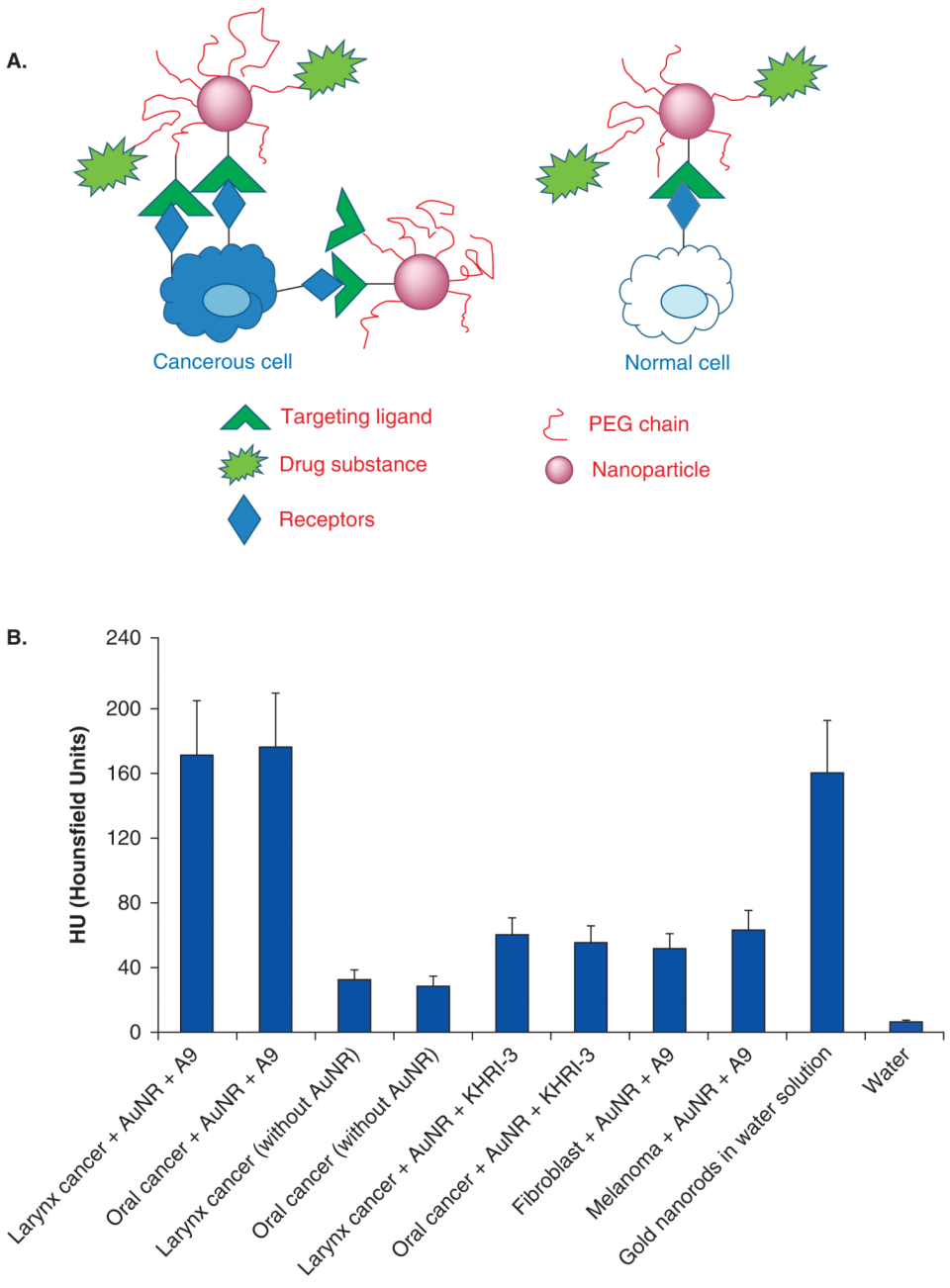

Figure 1.

A. Illustration of targeting cancerous cells with nanoparticles. **B.** CT attenuation (HU) of A9-antibody-coated gold nanorods (AuNR) with various cancerous and non-cancerous cells. Reproduced with permission from [16].

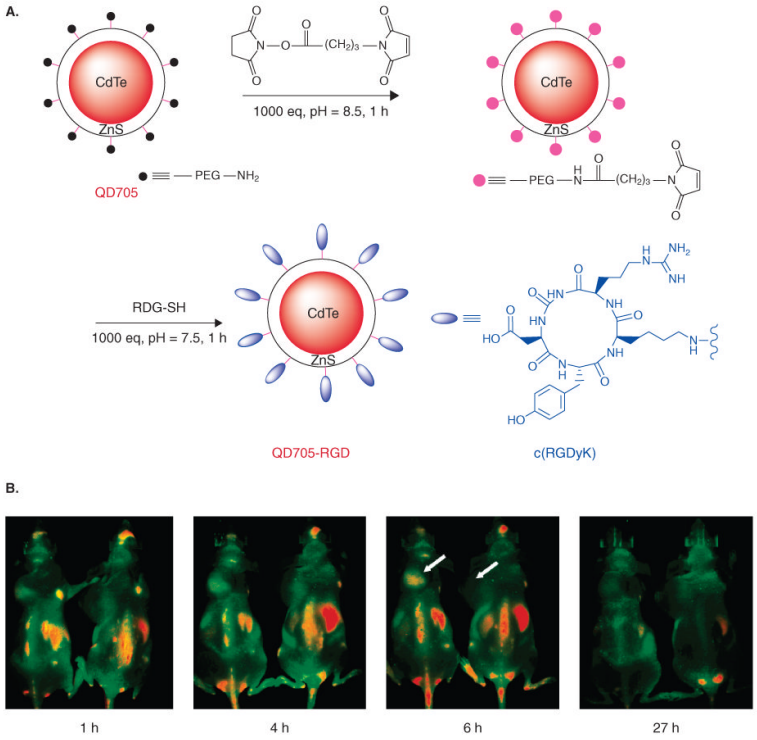

Figure 2.

A. Bioconjugation of QD705 and RGD peptide. **B.** *In vivo* fluorescence image of mice with U87MG tumor treated with QD705-RGD (left) and QD705 (right), respectively. Reproduced with permission from [67].

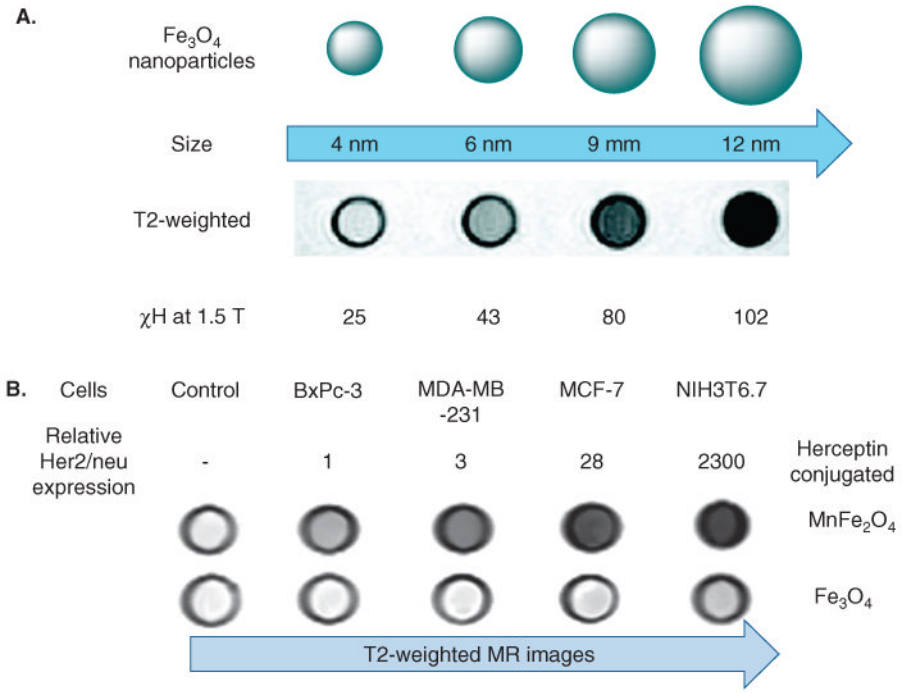

Figure 3.

A. Illustration of size-dependent T2-weighted images and mass magnetization of iron oxide nanoparticles at 1.5 T. **B.** Magnetic resonance contrast T2-weighed images with different HER2/neu expression levels.

A. Reproduced with permission from [96]. **B.** Reproduced with permission from [98].

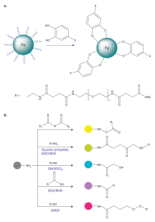

Figure 4.

A. Bioconjugation of iron oxide nanoparticles using bifunctional ligands. **B.** Bioconjugation of amino-CLIO-FITC with various small molecules.

Reproduced with permission from [103].

CLIO: Crosslinked iron oxide nanoparticles; FITC: Fluorescein isothiocyanate.

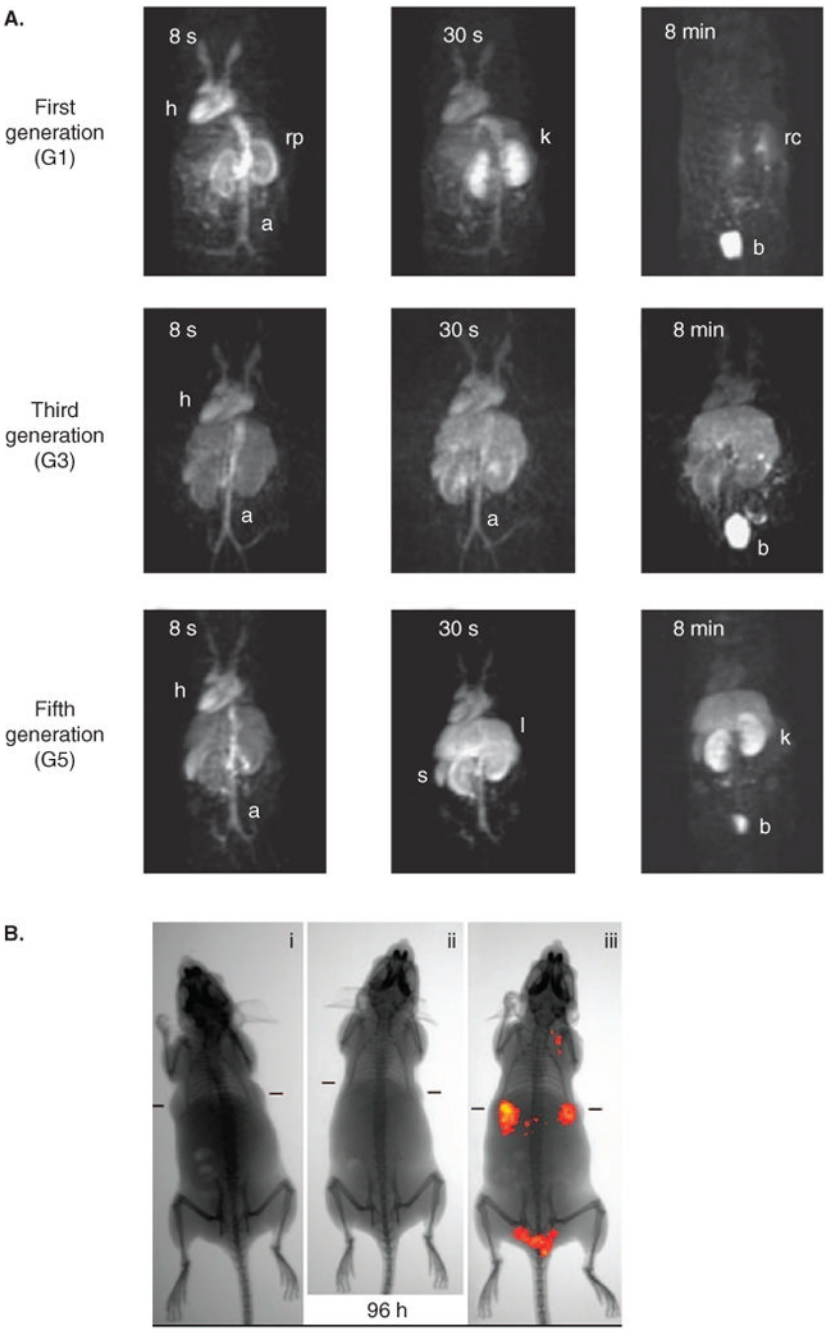

Figure 5.

A. MRI image of mice injected with first (G1), third (G3) and fifth (G5) generation Gd(III)-DTPA-PPI dendrimers. **B.** Near infrared transillumination images of ICG-CPNPs in nude mice implanted with human breast tumors.

A. Reproduced with permission from [133]. **B.** Reproduced with permission from [165].

CPNPs: Calcium phosphate nanoparticles; ICG: Indocyanine green.